Collisionless dynamics of the superconducting gap excited by a spin-splitting field

V. Plastovets [1,2] A. S. Mel'nikov,[2,3,4] and A. I. Buzdin[1,5]

[1] *University of Bordeaux, LOMA UMR-CNRS 5798, F-33405 Talence Cedex, France*
[2] *Institute for Physics of Microstructures, Russian Academy of Sciences, 603950 Nizhny Novgorod, GSP-105, Russia*
[3] *Moscow Institute of Physics and Technology, 141701 Dolgoprudny, Russia*
[4] *Lobachevsky State University of Nizhny Novgorod, 603950 Nizhni Novgorod, Russia*
[5] *World-Class Research Center "Digital Biodesign and Personalized Healthcare," Sechenov First Moscow State Medical University, 119991 Moscow, Russia*

(Received 12 May 2023; revised 23 August 2023; accepted 18 September 2023; published 27 September 2023)

We study the coherent dynamic interaction of a time-dependent spin-splitting field with the homogeneous superconducting order parameter $\Delta(t)$ mediated by spin-orbit coupling using the time-dependent Bogoliubov–de Gennes theory. *In the first part* of the work we show that the linear response of the superconductor is strongly affected by the Zeeman field and spin-flip processes, giving rise to multiple resonant frequencies of the superconducting Higgs modes, which can be coupled linearly to the fluctuating part of the Zeeman field. *In the second part*, we analyze the nonadiabatic dynamics of quasiparticle states arising from the intersection of spectral branches from different spin subbands provoked by a monotonically changing Zeeman field. Nonadiabatic spin-flip tunneling in the spectrum leads to drastic change in the order parameter $\Delta(t)$ above the Pauli limit and results in a nonequilibrium magnetization of the quasiparticle gas.

DOI: 10.1103/PhysRevB.108.104507

I. INTRODUCTION

Extensive studies of nonequilibrium states of superconductors [1,2] pay considerable attention to the so-called collisionless dynamics of a superconducting condensate, described by the complex-valued pairing potential $\Delta(t)$. At timescales shorter than the typical inelastic relaxation time $t \ll \tau_\varepsilon$ the dynamics of Cooper pairs is in coherent regime and is described by the Keldysh technique for Green's functions or its quasiclassical approximation [3,4]. The collisionless regime manifests itself most clearly in the existence of oscillations of the amplitude of the order parameter $\Delta(t) = \Delta_0 + \delta\Delta(t)$ near the equilibrium gap value Δ_0 (so-called Higgs mode [5,6]). This mode comes from excited interference interaction between the wave functions of the quasiparticles (QP) from broken Cooper pairs. Due to the QP dispersion, the summation over all interference contributions results in an inhomogeneous broadening of the total gap mode, which is equivalent to a weak damping with a typical time evolution $\delta\Delta(t) \propto \cos(2\Delta_0 t)/\sqrt{\Delta_0 t}$ [3]. Since the Higgs mode is a scalar excitation, it can not be coupled to the electromagnetic field $\mathbf{A}(t)$ linearly and several indirect mechanisms have been studied, such as a linear excitation by the THz radiation in the presence of dc supercurrent [7,8] and nonlinear coherent (or incoherent [9]) excitation by intense THz pulses, which can be detected by ultrafast pump-probe spectroscopy and third harmonic generation measurements [10–14].

It is known that, in addition to electromagnetic fields, superconductors also respond to nonstationary spin-splitting fields $\mathbf{h}(t)$. Typically, this field is produced by an external magnetic field $\mathbf{h} = \mu_B\mathbf{H}$ or by the exchange field of an adjacent ferromagnetic layer $\mathbf{h} \propto J_{\rm ex}\mathbf{M}_F$, which is induced by proximity to the superconductor. Spin-split systems serve as a good platform for spintronic applications and extensive study of various nonequilibrium processes has been done over the last few decades [15–17]. In particular, by inducing magnetic moment dynamics in superconductor-ferromagnet (S/F) junctions an effective spin-triplet component of the superconducting gap is generated resulting in long-range proximity effects [18–21]. On the other hand, experimental observations indicate that the superconducting subsystem has a direct impact on the ferromagnetic resonance in hybrid S/F structures [22–24].

In recent years there has been a growing interest in studying of the Higgs modes in the proximitized superconducting systems [25,26] as well as the interaction of collective modes in S/F systems [27]. For instance, it was recently shown that in a superconductor in the helical phase, which can be achieved in the presence of a strong spin-orbit coupling (SOC) and an exchange field, the Higgs mode can be linearly coupled to the electromagnetic field through the nonzero superconducting phase gradient in the ground state [28]. Also, it was revealed that the coupling of the Higgs mode $\delta\Delta(t)$ in a superconductor to external light $\mathbf{A}(t)$ and magnetic dynamics $\mathbf{m}(t)$ in the F layer allows the generation of time-dependent spin currents [29]. These currents can themselves excite the Higgs mode in the superconductor through the resonance of the ferromagnet due to the reciprocal effect [29]. Another example is an interplay between the superconducting Higgs mode and a magnon mode in the adjacent F layer in the presence of a SOC and static proximity effect [30]. Interestingly, the Higgs mode here is coupled to the Zeeman field $\mathbf{h}(t)$ linearly due to the presence of both the spin-orbit interaction and some preferred direction given by wave vector of the magnetic mode.

According to the aforementioned works, the SOC is critical for interaction of different spin subbands of the QP spectrum, which directly leads to the gap dynamics $\Delta(t)$. Some preconditions for this can be taken from the elementary analysis of the equilibrium state. The equilibrium superconducting gap does not depend on the Zeeman field below the so-called paramagnetic limit $h_{\rm cr} = \Delta_0/\sqrt{2}$, so that $\Delta(h < h_{\rm cr}, T = 0) = \Delta_0$; and above this limit the superconductivity is completely suppressed with $\Delta(h > h_{\rm cr}, T = 0) = 0$ [31,32]. The SOC drastically changes the dependence $\Delta(h)$ and promotes a generation of triplet component superconducting correlations, leading to the survival of the gap at $h > h_{\rm cr}$ [33]. This effect is associated with mixing of the different spin states of QP, which is natural to expect in the nonstationary case as well.

The purpose of this work is to study the dynamical aspects of the nonequilibrium state of a superconducting condensate excited in the presence of both a spin-splitting field and SOC. For the sake of simplicity we consider specific system of a uniform superconductor at zero temperature $T = 0$ and consider short timescale $t \ll \tau_\varepsilon$ at which the collisionless regime holds, so one can treat the system with the pure quantum-mechanical approach within the time-dependent Bogoliubov–de Gennes (TDBdG) equations [34]. We assume a homogeneous SOC and a spin-splitting field with only one component $\mathbf{h}(t) = h(t)\mathbf{z}_0$.

After introducing the TDBdG equations in Sec. II, we examine two different regimes of coherent evolution of the order parameter. In Sec. III we analyze linearized gap dynamics where the temporal evolution of the Higgs modes $\delta\Delta(t)$ is traced in the presence of a stationary spin-splitting field h_0. Since the SOC allows the transitions between the QP states with different spins, the induced perturbation of the gap $\delta\Delta(t)$ acquires three eigenfrequencies including the standard $2\Delta_0$ and two additional frequencies $2(\Delta_0 \pm h_0)$. These modes define both the free oscillation of the perturbed gap at $h_0^{-1} \ll t \ll \tau_\varepsilon$, and resonant peaks in the case of driven oscillations. It was also shown that in the specific configuration, the linear coupling of the Higgs mode and the perturbation of the Zeeman field $\delta\mathbf{h}(t)$ codirectional with $\mathbf{h}_0$ is possible. Note that the frequencies shifted by the spin-splitting field have been observed in the numerical simulation of the dynamics of the one-dimensional Fermi superfluid exposed to the nonstationary Zeeman field and strong SOC in Ref. [35].

In Sec. IV we consider the dynamics of the gap $\Delta(t)$ driven out of equilibrium by linearly growing field $\mathbf{h}(t)$. At some point the field becomes larger then the equilibrium gap value $|\mathbf{h}(t)| > \Delta_0$ and thus provokes the crossing of the branches from different spin subbands of the QP spectrum. The appearance of nonadiabatic transitions between the states at the intersection point is equivalent to the dynamical spin-flip process and can be described with the Landau-Zener-Stückelberg-Majorana (LZSM) tunneling problem [36]. Corresponding redistribution of QP states contributes to the gap function $\Delta(t)$ and drastically changes its behavior depending on the field growth rate. In Secs. IV C and IV D we derive an analytical expression for $\Delta(t)$ from the self-consistency equation which contains two different terms: (i) quasistatic dependence $\Delta_h[h(t)]$ arising directly from spin-flip tunneling and depending on the probability of redistribution of QP states; (ii) small oscillating part $\delta\Delta(t)$ originating from the interference between redistributed states. In addition, in Secs. IV E and IV F we discussed the spin imbalance generated due to LZSM tunneling and corresponding dynamical magnetization of the QP gas. Some experimental proposals and conclusions are presented in Secs. V and Sec. VI. respectively.

II. TIME-DEPENDENT BOGOLIUBOV–de GENNES EQUATIONS

We consider a homogeneous s-wave superconductor in the presence of the uniform time-dependent Zeeman field $h(t)$ and Rashba spin-orbit coupling (RSOC). The coherent QP dynamics is governed by the TDBdG equations [34]

$$i\frac{\partial}{\partial t}\check{\psi}_k = \check{\mathcal{H}}(k,t)\check{\psi}_k, \tag{1}$$

where the Hamiltonian

$$\check{\mathcal{H}}(k,t) = \begin{pmatrix} \hat{H}(k,t) & i\hat{\sigma}_y\Delta(t) \\ -i\hat{\sigma}_y\Delta(t) & -\hat{H}^*(-k,t) \end{pmatrix} \tag{2}$$

is the 4×4 matrix in the Nambu $\times$ spin space with the Pauli matrices $\hat{\sigma}_i$ acting on the four-component wave function $\check{\psi}_k(t)$. The single-particle matrix Hamiltonian in the spin space $\hat{H}(k,t) = \xi_k\hat{\sigma}_0 - h(t)\mathbf{z}_0\hat{\boldsymbol{\sigma}} + \alpha(\hat{\boldsymbol{\sigma}} \times \mathbf{k})\mathbf{z}_0$ depends on the modulus $k = |\mathbf{k}|$ and the relative phase $\theta_k = \arg(k_x + ik_y)$ of the momentum. Here $\xi_k = k^2/2m - E_F$ is a free-particle spectrum measured from the Fermi level and α is a strength of RSOC. Hereafter, we put $\hbar = 1$. For simplicity we consider here the motion of QPs only in the x-y plane neglecting their dispersion along the $\mathbf{z}_0$ axis, so that $\mathbf{k} = (k_x, k_y)$.

The pairing potential $\Delta(t)$ should satisfy the self-consistency equation, which at zero temperature $T = 0$ can be written as

$$\Delta(t) = -\frac{\lambda}{2}\sum_{\rm i.c.}\check{\psi}_k^\dagger(t)\check{\tau}_\Delta\check{\psi}_k(t), \tag{3}$$

where λ is the pairing constant, $\check{\tau}_\Delta = (\hat{\tau}_x + i\hat{\tau}_y) \otimes i\hat{\sigma}_y/2$, and the independence of Δ on θ_k is taken into account. The summation here is performed over all solutions of Eq. (1) for different initial conditions (i.c.) at $t = 0$. The information about the dynamics as well as the distribution function of the QP excitations is contained in the functions $\check{\psi}_k(t)$, which self-consistently define the temporal evolution of the gap. In the homogeneous problem, the initial conditions are numbered by the momentum k, which, in the case of a spin-split superconductor, must be supplemented by the spin quantum number. All possible initial configurations of the QP states are defined by an equilibrium distribution function. The pairing potential $\Delta(t)$ can be chosen as a real function of time, and this choice will be justified below.

Generally speaking, the concept of an energy spectrum for a dynamical system is not clearly defined. However, in the case of adiabatic evolution one can introduce the eikonal approximation for the QP wave functions $\check{\psi}_k(t) \propto \check{\Psi}_k(t)e^{iS_k(t)}$, from which the adiabatic spectrum $E_k(t) = -\partial_t S_k$ can be extracted. The functions $\check{\Psi}_k(t)$ are the instantaneous eigenstates of the Hamiltonian $\check{\mathcal{H}}(t)$ from Eq. (2). The resulting spectrum is

$$E_{kn}(t) = \pm\sqrt{E_0^2 + \alpha^2k^2 + h^2(t) \mp \mathrm{sgn}(\sigma)2\sqrt{\xi_k^2\alpha^2k^2 + h^2(t)E_0^2}}, \tag{4}$$

where $E_0 = \sqrt{\xi_k^2 + \Delta^2}$. We use the index $n \equiv \sigma\pm = \{\uparrow+, \downarrow+, \uparrow-, \downarrow-\}$ which refers to different spin subbands and positive and negative energies (these notations will be used in the text below). There are four corresponding instantaneous eigenstates which can be written as $\check{\Psi}_{kn}(t) = (u_{k\uparrow n}, u_{k\downarrow n}, v_{k\uparrow n}, v_{k\downarrow n})^T$. The detailed structure of the vectors is given in Appendix A. The functions $\check{\Psi}_{kn}(t)$ form an orthonormal basis with the normalization condition $\check{\Psi}^\dagger_{kn}\check{\Psi}_{kn'} = \delta_{nn'}$ and the completeness relation $\sum_{kn}\check{\Psi}_{kn}\check{\Psi}^\dagger_{kn} = \check{1}$. Obviously, in the limit of the stationary Zeeman field, $\check{\Psi}_{kn}$ becomes an exact solution of stationary problem (1).

It is important to keep in mind that in the presence of both RSOC and spin-splitting field the equilibrium gap value depends of the values of these fields $\Delta_{\rm eq} = \Delta_{\rm eq}(h, \alpha)$. In what follows, the RSOC strength α will be considered as a small parameter, and the static dependence $\Delta(\alpha)$ will be neglected for simplicity. Thus, the equilibrium gap value is defined as follows:

$$\Delta_{\rm eq} = \Delta_0 = 2\hbar\omega_D e^{-\frac{1}{\lambda N(0)}},$$

where ω_D is Debye frequency and $N(0)$ is the density of states at Fermi energy.

III. LINEARIZED GAP DYNAMICS

In this section we want to address the temporal evolution of a small fluctuation of the gap $\Delta_0 + \delta\Delta(t)$ in the presence of the static spin-splitting field $\mathbf{h} = h_0\mathbf{z}_0$. The gap dynamics can be excited by some external pulse at $t = 0$ or can be driven, for instance, by time-dependent spin-splitting field $\delta\mathbf{h}(t) = \delta h(t)\mathbf{z}_0$. In linear order in small perturbations $\delta\Delta(t)$, $\delta h(t) \ll h_0 < \Delta_0$, the TDBdG equations for the QP wave functions read as

$$i\frac{\partial}{\partial t}\check{\psi}_k(t) = [\check{\mathcal{H}}_0 + \check{\mathcal{V}}(t)]\check{\psi}_k(t), \tag{5}$$

where the operators in the Nambu × spin space are

$$\check{\mathcal{H}}_0 = \begin{pmatrix} \hat{H}_0(k) & i\hat{\sigma}_y\Delta_0 \\ -i\hat{\sigma}_y\Delta_0 & -\hat{H}_0^*(-k) \end{pmatrix},$$
$$\check{\mathcal{V}}(t) = \begin{pmatrix} -\delta h(t)\hat{\sigma}_z & i\hat{\sigma}_y\delta\Delta(t) \\ -i\hat{\sigma}_y\delta\Delta(t) & -\delta h(t)\hat{\sigma}_z \end{pmatrix}, \tag{6}$$

and single-particle Hamiltonian is $\hat{H}_0(k) = \xi_k\hat{\sigma}_0 - h_0\hat{\sigma}_z + \alpha(k_y\hat{\sigma}_x - k_x\hat{\sigma}_y)$.

Time-dependent equation (5) can be written in the adiabatic basis using stationary eigenfunctions $\check{\Psi}_{kn}$ of the operator $\check{\mathcal{H}}_0$. Additionally, the RSOC energy $\alpha k \approx \alpha k_F$ is considered a perturbative parameter. By approximating the eigenvectors up to first order in $\alpha k_F/\Delta_0$ (see Appendix A), we can infer from Eq. (3) that the fluctuation in the gap will have an order up to $O(\alpha^2 k_F^2/\Delta_0^2)$. However, in the general case, the gap Δ should not be affected by the direction of the SOC. Therefore, the first-order change in the gap $\delta\Delta \propto O(\alpha k_F/\Delta_0)$ must vanish.

Instead of the general eikonal theory, we use the perturbative approach with the ansatz written in terms of the dynamical phase

$$\check{\psi}_k(t) = \sum_n \check{\Psi}_{kn}C_{kn}(t)e^{-iE_{kn}t}. \tag{7}$$

The index $n = \{\uparrow +, \downarrow +, \uparrow -, \downarrow -\}$ denotes the spectral branches and all negative and positive energy terms are involved into the dynamics of QPs. Substituting the function (7) into Eq. (5) we obtain the equation for the dynamics of the coefficients

$$i\frac{\partial}{\partial t}C_{km}(t) = \sum_n \check{\Psi}^\dagger_m\check{\mathcal{V}}(t)\check{\Psi}_n e^{-i(E_n - E_m)t}C_{kn}(t), \tag{8}$$

which completely determine the evolution of gap $\Delta(t)$ in time through the self-consistency equation

$$\Delta_0 + \delta\Delta(t) = -\frac{\lambda}{2}\sum_{\rm i.c.}\sum_{n,n'} C^*_{kn}(t)C_{kn'}(t)e^{-i(E_{n'} - E_n)t}\check{\Psi}^\dagger_{kn}\check{\tau}_\Delta\check{\Psi}_{kn'}. \tag{9}$$

The dynamics of the system is considered in the interval $t \in [0, \infty)$.

Equation (8) describes transitions between the states with different n. The conservation of k simplifies the formulation of the initial conditions. In the case of zero temperature $T = 0$ there are two possible initial configurations at $t = 0$. All QP states with energies below Fermi level in the first (second) spin subband with $\sigma = \uparrow$ ($\downarrow$) are fully occupied for all momenta with $\xi_k \in (-\omega_D, \omega_D)$. This imposes two corresponding initial conditions for Eq. (8):

$$\text{(i)}\quad C_{k\uparrow -}(0) = 1, \quad C_{k[\downarrow -, \uparrow +, \downarrow +]}(0) = 0;$$
$$\text{(ii)}\quad C_{k\downarrow -}(0) = 1, \quad C_{k[\uparrow -, \uparrow +, \downarrow +]}(0) = 0. \tag{10}$$

Therefore, it is natural to linearize Eq. (8) as follows:

$$C_{kn}(t) = C_{kn}(0) + \delta C_{kn}(t). \tag{11}$$

The sum in Eq. (9) should be taken over all QP states originating from the above i.c. (10).

Performing Laplace transform in the complex plane $s = i\omega + \zeta$ for the linearized equations (8), (9), and (11) (see Appendix B) we get the following dynamic self-consistency equation:

$$\delta\Delta(s) = [\mathcal{K}_0(s) + \mathcal{K}_+(s) + \mathcal{K}_-(s)]\delta\Delta(s) + [\mathcal{F}_+(s) - \mathcal{F}_-(s)]\delta h(s) + \mathcal{I}(s). \tag{12}$$

Here $\mathcal{K}_{0,\pm}(s)$ are kernels of the self-consistency equation and $\mathcal{F}_\pm(s)$ defines the dynamical structure of the "force" term (in analogy with a mechanical oscillator) related with $\delta h(t)$. The term $\mathcal{I}(s)$ [see Eq. (B8) in Appendix B] is determined by the initial nonequilibrium perturbation in the distribution of the QP population through the coefficients $\delta C_{kn}(t = 0)$. Taking into account Eq. (9) this term can be treated as an effective self-consistent initial condition for the gap dynamics $\delta\Delta(t)$. Due to the absence of particle-hole asymmetry, which couples the phase and amplitude fluctuations [6], the imaginary part of $\delta\Delta(s)$ naturally vanishes and we consider only amplitude (or Higgs) modes of the superconducting gap. Knowing the function $\mathcal{K}(s)$ one can find eigenfrequencies and free dynamics of the system, while $\mathcal{F}_\pm(s)$ induces the driven dynamics. We will conduct a thorough examination of these terms below.

A. Spin-split Higgs modes

It is known that in the absence of a spin-splitting field and RSOC the Higgs mode has a singular behavior in the vicinity of the eigenfrequency $\omega = 2\Delta_0$, which defines the free evolution of the gap perturbation $\delta\Delta(t) \propto \cos(2\Delta_0 t)/\sqrt{t}$ [14]. Since the energy of the Higgs mode lies at the lower bound of the QP spectrum, the oscillatory behavior here can be represented as a coherent decay and formation of a Cooper pair into two QPs with opposite spins and energies Δ_0 at $k \approx k_F$. The contribution from the pairs of QPs with other momenta leads to the inhomogeneous broadening of the mode with the corresponding damping law. The presence of Zeeman field and RSOC makes the dynamics more complicated. To analyze the eigenmodes of the superconductor one can set $\delta h(t) = 0$ and write the self-consistency equation as follows:

$$\chi^{-1}_{\Delta\Delta}(s)\delta\Delta(s) = \mathcal{I}(s), \tag{13}$$

where we define the bare pair susceptibility

$$\chi_{\Delta\Delta}(s) = \frac{1}{1 - \mathcal{K}_0(s) - \mathcal{K}_+(s) - \mathcal{K}_-(s)}. \tag{14}$$

The corresponding kernels read as (see Appendix B)

$$\mathcal{K}_0(s) = \left\langle \frac{2\xi^2}{E_0}\frac{1}{s^2 + 4E_0^2}\right\rangle \propto O\left(\frac{\alpha^0 k_F^0}{\Delta_0^0}\right),$$
$$\mathcal{K}_\pm(s) = \left\langle \mathcal{A}^2(\xi)\frac{E_0 \pm h_0}{s^2 + 4(E_0 \pm h_0)^2}\right\rangle \propto O\left(\frac{\alpha^2 k_F^2}{\Delta_0^2}\right), \tag{15}$$

where the notation $\langle \dots \rangle = \lambda N(0)\int_{-\omega_D}^{\omega_D} d\xi$ is used. The function $\mathcal{A}(\xi) \propto \check{\Psi}^{0\dagger}_{kn}\check{\tau}_\Delta \check{\Psi}^0_{kn} \propto \alpha k_F/\Delta_0$ is proportional to nonzero triplet component of the wave function, therefore, the kernels $\mathcal{K}_\pm$ are of the second order in the RSOC parameter.

The frequencies of the eigenmodes of the superconducting condensate can be traced out from the condition $|\chi^{-1}_{\Delta\Delta}(\omega)| = 0$, which reflects the singular points of the kernels (15). Consider these points in more detail. Instead of straightforward integrating, we are going to implement the analysis in the spirit of the work [3] and analytically obtain the limit $\zeta \to 0$. The functions $\mathcal{K}_{0,\pm}(s \to \omega)$ can be represented as $\mathcal{K}(s) = \mathcal{K}'(\omega) + i\,\mathrm{sgn}(\omega\zeta)\mathcal{K}''(\omega)$. The real parts of the kernels

$$\frac{\mathcal{K}_0'(\omega)}{\lambda N(0)} = \int_{-\omega_D}^{\omega_D} \frac{2\xi^2}{\sqrt{\xi^2 + \Delta_0^2}(4\xi^2 + 4\Delta_0^2 - \omega^2)}d\xi, \tag{16}$$

$$\frac{\mathcal{K}_\pm'(\omega)}{\lambda N(0)} = \int_{-\omega_D}^{\omega_D} \frac{\mathcal{A}^2(\xi)(E_0 \pm h_0)}{4(E_0 - h_0)^2 \pm |\omega|^2}d\xi \tag{17}$$

are regular on the imaginary axis $s = i\omega$. The imaginary parts are

$$\frac{\mathcal{K}_0''(\omega)}{\lambda N(0)} = -\frac{\pi}{2}\frac{\sqrt{\omega^2 - \omega_0^2}}{|\omega|}\Theta\left[\omega^2 - \omega_0^2\right], \tag{18}$$

$$\frac{\mathcal{K}_\pm''(\omega)}{\lambda N(0)} = -\frac{\pi}{8}\frac{|\omega| \mp 2h_0}{\xi_\pm}\mathcal{A}^2(\xi_\pm)\Theta\left[\omega^2 - \omega_\pm^2\right], \tag{19}$$

where $\xi_\pm = \frac{1}{2}\sqrt{(|\omega| - \omega_\pm)^2 + 4\Delta_0(|\omega| - \omega_\pm)}$. The discontinuities at the real axis ζ mean the existence of the branch points

$$\omega_0 = 2\Delta_0, \quad \omega_+ = 2(\Delta_0 + h_0), \quad \omega_- = 2(\Delta_0 - h_0), \tag{20}$$

and corresponding cuts in the complex plane [Fig. 1(a)].

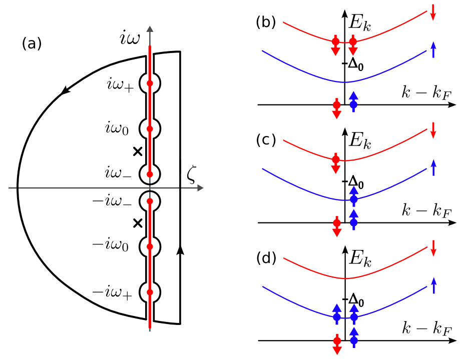

FIG. 1. (a) Branch points $\omega_0 = 2\Delta_0, \omega_\pm = 2(\Delta_0 \pm h_0)$ (red dots) corresponding to the kernels $\mathcal{K}_0(s)$ and $\mathcal{K}_\pm(s)$, $\mathcal{F}_\pm(s)$ [Eq. (12)] in the complex plane $s = i\omega + \zeta$. Red lines show the chosen branch cuts. Black crosses correspond to the poles of the external force $\delta h(s)$. (b)–(d) Illustration of physical mechanism behind the appearance of three eigenfrequencies ω_+ (b), ω_0 (c), ω_- (d).

The analysis of the general linear response of the order parameter can be significantly simplified by expanding the susceptibility $|\chi_{\Delta\Delta}(\omega)|$ in the powers of the small parameter $\alpha k_F/\Delta_0$ since the kernels $\mathcal{K}_\pm \propto O(\alpha^2 k_F^2/\Delta_0^2)$. As mentioned before, the maximum order we can take into account is $|\chi_{\Delta\Delta}| \propto O(\alpha^2 k_F^2/\Delta_0^2)$. The resonance condition $|\chi^{-1}_{\Delta\Delta}(\omega)| = 0$ is satisfied at $\omega = \omega_\pm$ where the kernels $\mathcal{K}_\pm''(s)$ have a singularity (note that $\mathcal{A}$ is regular at $\xi = \xi_\pm$), and at $\omega = \omega_0$, where the function $\mathcal{K}_0''(s)$ goes to zero. Thus, the branch points (20) define new eigenmodes of the superconductor in the presence of spin-splitting field and weak RSOC.

One can obtain an asymptotic behavior these eigenmodes in the time domain [3]. Let us assume the specific form of the initial condition $\mathcal{I}(s) = \mathcal{I}_0 = \text{const}$ in Eq. (12), which corresponds to a certain quench. We consider the impulse response of the gap fluctuation for $t \in [0, \infty)$ using inverse Laplace transform

$$\delta\Delta(t) = \frac{1}{2\pi i}\int_{-i\infty+\epsilon}^{i\infty+\epsilon} \chi_{\Delta\Delta}(s)\mathcal{I}_0 e^{st}ds. \tag{21}$$

The integral can be evaluated using closed contour shown in Fig. 1(a). Making sure that all integrals on infinitely large and small arcs vanish and applying residue theorem we get

$$\delta\Delta(t) = \frac{2}{\pi}\int_{\omega_-}^{\infty} \mathrm{Im}\chi_{\Delta\Delta}(s)|_{\zeta\to+0}\mathrm{Im}[e^{i\omega t}\mathcal{I}_0]d\omega. \tag{22}$$

One can show that the peculiarities in the vicinities of the eigenfrequencies in $\mathrm{Im}\chi_{\Delta\Delta}(s)$ lead to three partial contributions to the long-time ($h_0^{-1} \ll t$) gap dynamics

$$\delta\Delta(t) \approx \frac{4\Delta_0}{\pi^{3/2}}\frac{\mathcal{I}_0}{\lambda N(0)}\frac{\cos(\omega_0 t - \pi/4)}{\sqrt{\Delta_0 t}}$$
$$- \frac{\sqrt{\pi}}{2}\frac{(\alpha k_F)^2\Delta_0}{(\Delta_0 - h_0)^2}\sum_{j=\pm}\frac{\lambda N(0)\mathcal{I}_0}{|1 - \mathcal{K}_0(\omega_j)|^2}\frac{\cos(\omega_j t - \pi/4)}{\sqrt{\Delta_0 t}}, \tag{23}$$

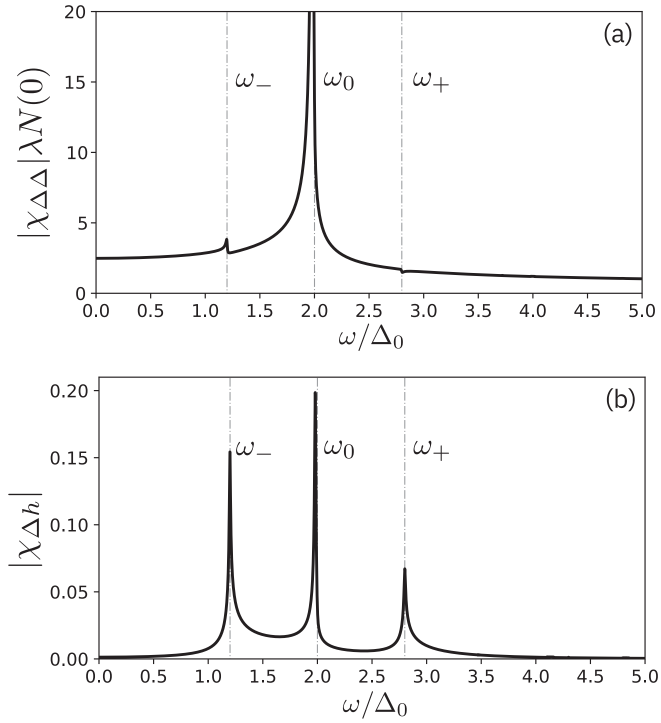

FIG. 2. (a) The bare pair susceptibility $|\chi_{\Delta\Delta}(s)|$ from Eq. (14) for $s = i\omega + \zeta$. Features at the frequencies $\omega_0 = 2\Delta_0$ and $\omega_\pm = 2(\Delta_0 \pm h_0)$ correspond to Higgs modes resonances. (b) Response function $|\chi_{\Delta h}(s)|$ of the driven gap oscillations $\delta\Delta(t)$ excited by the Zeeman field $\delta h(t)$. Both plots are symmetrical with respect to $\omega \to -\omega$ and have the parameters $h_0 = 0.4\Delta_0$, $\alpha k_F = 0.09\Delta_0$. Broadening of the resonance peaks is given by $\zeta = 0.005\Delta_0$.

which can be identified as spin-split Higgs modes. Details of the derivation of $\delta\Delta(t)$ are provided in Appendix C.

Appearance of the frequencies (20) and corresponding oscillations (23) in the spin-split superconductor can be explained qualitatively. Coherent decay of the Cooper pairs from the Fermi level can occur into two different spin subbands of the QP spectrum. When two electrons with opposite spins from a pair dissociate into two QP at $k \approx k_F$ with the energies $\Delta_0 \pm h_0$ without spin flipping, then the total decay energy is equal to QP threshold $\approx 2\Delta_0$. This process corresponds to the mode $2\Delta_0$ and shown in Fig. 1(c). A decay into two QPs with the same spins is possible in the presence of RSOC due to the effective spin-flip scattering. The energies of such two QPs are either $\Delta_0 + h_0$ or $\Delta_0 - h_0$. This process leads to the modes $2(\Delta_0 \pm h_0)$ correspondingly [Figs. 1(b) and 1(d)]. Note that this naive interpretation of the complicated QP dynamics is valid for the sufficiently small RSOC $\alpha k_F \ll \Delta_0$.

Numerically calculated susceptibility $|\chi_{\Delta\Delta}(\omega)|$ from Eqs. (14) and (15) is shown in Fig. 2(a). The observed resonances have a different parametric order of smallness. The Higgs mode with the frequency ω_0 which exists in the absent the RCOS becomes dominating with more pronounced peak $|\chi_{\Delta\Delta}(\omega \approx \omega_0)| \propto \alpha^0 k_F^0$, whereas two other modes at shifted frequencies $\omega_\pm$ are of the order of $|\chi_{\Delta\Delta}(\omega \approx \omega_\pm)| \propto \alpha^2 k_F^2/\Delta_0^2$. These modes merge with ω_0 at $h_0 \to 0$ and disappear for $\alpha \to 0$. It is expected that the excitation of the bare response of the superconductor can be implemented with the standard THz laser pump-probe techniques. The electric field of the pump pulse produces a quench of the spin-split superconductor and subsequent probe pulse detects the multifrequency Higgs oscillations.

Note that a similar dynamics of the order parameter was studied in the spin-orbit coupled Fermi gases [37–39]. In particular, the existence of the Higgs modes modified by the Zeeman field in the presence of strong SOC with $\alpha k_F \sim h(t) \sim E_F$ was discussed in Ref. [35]. The authors performed a numerical simulation of the one-dimensional Fermi superfluid and examined the excitation of the gap oscillations with few frequencies by abrupt change of the Zeeman field. Despite the significant differences between the models, there is a general tendency for the influence of the shift of spectral QP branches on the behavior of the order parameter modes.

We also note that in the presence of the strong Zeeman field the superconductor can be unstable to a transition to the spatially modulated Fulde-Ferrell-Larkin-Ovchinnikov (FFLO) state with inhomogeneous order parameter. The appearance of the broken translational symmetry gives rise to gapless Higgs and Goldstone modes, which have been investigated theoretically in Refs. [40,41]. Hereafter we ignored the possibility of of FFLO formation, focusing on purely homogeneous case.

B. Coupling of Higgs modes and Zeeman field

We found that, in addition to an electromagnetic field, the gap dynamics in a spin-split superconductor can be excited by a nonstationary component of Zeeman field $\mathbf{h}(t) = [h_0 + \delta h(t)]\mathbf{z}_0$. In this particular configuration the perturbation of the spin-splitting field $\delta h(t)$ appears in the self-consistency equation (12) in the first order, which is the trace of a dot product $(\mathbf{h}_0 \cdot \delta\mathbf{h})$. Note that the field $\delta h(s)$ is weighted by the functions

$$\mathcal{F}_\pm(s) = \left\langle \mathcal{A}(\xi)\mathcal{B}(\xi)\frac{(E_0 \pm h_0)}{s^2 + 4(E_0 \pm h_0)^2} \right\rangle \propto O\left(\frac{\alpha^2 k_F^2}{\Delta_0^2}\right), \quad (24)$$

which can be written as $\mathcal{F}(s) = \mathcal{F}'(\omega) + i\,\mathrm{sgn}(\omega\zeta)\mathcal{F}''(\omega)$ and have the same order in αk_F and the same analytical properties as the kernels $\mathcal{K}_\pm(s)$ in (17) and (19) because both functions $\mathcal{A}^2(\xi)$ and $\mathcal{A}(\xi)\mathcal{B}(\xi)$ are regular for $\xi \in (-\omega_D, \omega_D)$. The presence of the singular points in the force term makes the analysis of Eq. (12) more sophisticated, despite the fact that these points are shared with other kernels.

Consider the general case of forced oscillations of the order parameter driven by some field $\delta h(t)$ which is abruptly turned on at $t = 0$. It is convenient to introduce the linear response function as follows:

$$\delta\Delta(s) = \chi_{\Delta h}(s)\delta h(s), \quad (25)$$

$$\chi_{\Delta h}(s) = \frac{\mathcal{F}_+(s) - \mathcal{F}_-(s)}{1 - \mathcal{K}_0(s) - \mathcal{K}_+(s) - \mathcal{K}_-(s)}. \quad (26)$$

The numerically integrated shape of $|\chi_{\Delta h}(s)|$ is shown in Fig. 2(b) and, as expected, it has three resonance peaks at the frequencies $\omega_{0,\pm}$. However, since the external field $\delta\mathbf{h}(t)$ couples to the gap through the RSOC, the amplitude of the susceptibility in the vicinity of the resonances has the same order of smallness $|\chi_{\Delta h}(\omega_{0,\pm})| \propto O(\alpha^2 k_F^2/\Delta_0^2)$, which differs from the bare response (14).

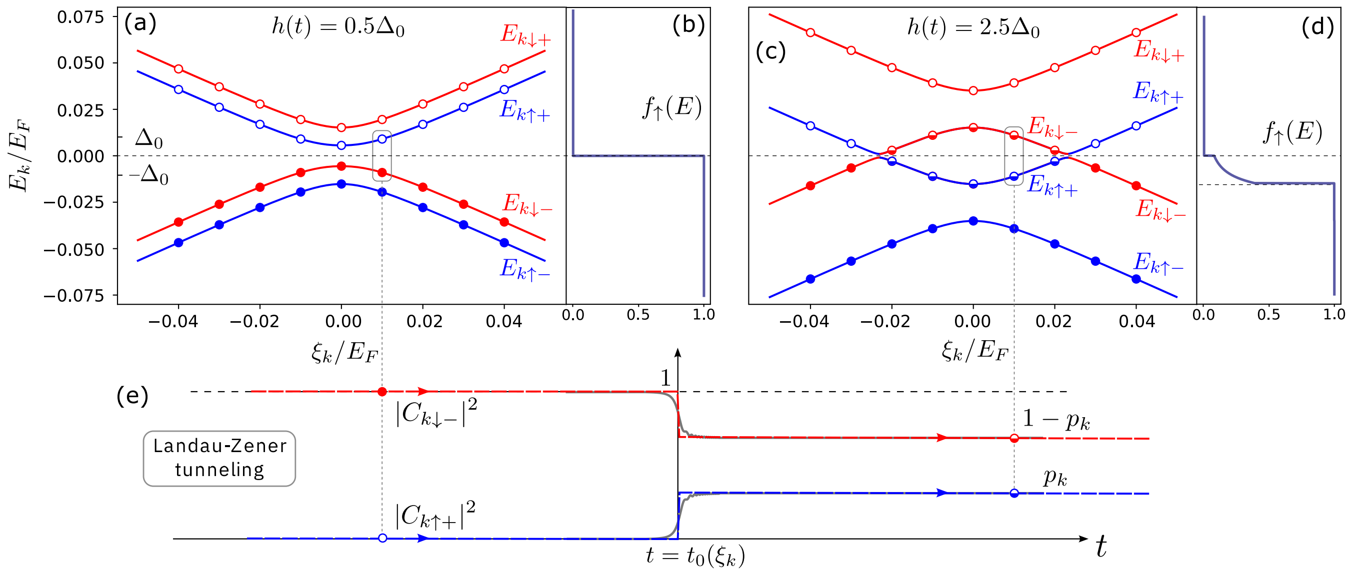

FIG. 3. (a), (b) QP spectrum E_k from Eq. (4) for $\Delta_0/E_F = 0.01$, $\alpha k_F/E_F = 0.0025$, and for two values of Zeeman field $h(t)$ before (a) and after (b) avoided crossing. Colored (empty) circles correspond to filled (empty) states. In (e) the schematic temporal evolution of the filling probabilities $|C_k|^2(t)$ for two states at fixed ξ_k is shown. The gray lines show a tunneling process similar to the real one in the vicinity of the avoided transition point $t_0(\xi_k) = \sqrt{\xi_k^2 + \Delta_0^2}/\gamma$, while red and blue lines refer to transition matrix approximation of the LZSM tunneling with the probability p_k. (b), (d) The QP distribution function for one spin projection $f_\uparrow(E, t)$ from Eq. (45) before and after crossing of spectral branches at $\delta_{\rm LZ} = 0.5$.

The temporal evolution of the gap fluctuation $\delta\Delta(t)$ in $[0, \infty)$ can be found using inverse Laplace transform. Similarly to Eq. (22) the susceptibility ${\rm Im}\chi_{\Delta h}$ can be expanded into series since $\mathcal{F}_\pm, \mathcal{K}_\pm \propto O(\alpha^2 k_F^2/\Delta_0^2)$, and different strongly dominant terms in the vicinity of the branch points (20) can be distinguished (Fig. 2). Here we write the result for the superconducting gap oscillations, which at large times $h_0^{-1} \ll t$ reads as (for details see Appendix C)

$$\delta\Delta(t) \approx \sum_p \chi_{\Delta h}(s_p) e^{s_p t} \underset{s=s_p}{\rm Res}[\delta h(s)] + \frac{4\Delta_0}{\pi^{3/2}} \frac{[\mathcal{F}_+'(\omega_0) - \mathcal{F}_-'(\omega_0)]}{\lambda N(0)} \frac{{\rm Im}[\delta h(i\omega_0) e^{i(\omega_0 t + \pi/4)}]}{\sqrt{\Delta_0 t}}$$
$$+ \frac{\sqrt{\pi}}{2} \frac{(\alpha k_F)^2 \Delta_0}{(\Delta_0 - h_0)^2} \sum_{j=\pm} \frac{\lambda N(0)[1 - \mathcal{K}_0'(\omega_j)]}{|1 - \mathcal{K}_0(\omega_j)|^2} \frac{{\rm Im}[\delta h(i\omega_j) e^{i(\omega_j t + \pi/4)}]}{\sqrt{\Delta_0 t}}. \tag{27}$$

The first term here is related to the forced oscillations of the gap, caused by the Zeeman field $\delta h(t)$. For instance, the general harmonic perturbation $\delta h(t) = {\rm Re}(\delta h_0 e^{(i\omega - \beta)t})$ with $\beta \to 0$ yields two poles s_p shown in Fig. 1(a). The last three terms in (27) correspond to the free oscillations triggered by $\delta h(t)$ at $t = 0$ in the long-time asymptote, with three characteristic frequencies (20) and square-root damping law. The latter can be interpreted as partial contribution from the Higgs modes in the spin-splitting field h_0. The eigenmodes decay at $t \to \infty$ and in the long-time asymptote the forced oscillations prevail. Consider the steady-state behavior of $\delta\Delta(t)$ [the first term in Eq. (27)] in the time interval restricted by the inelastic relaxation processes where the presented description of the coherent gap dynamics is valid.

In this section, we have solely focused on the longitudinal component of the field perturbation $\delta h(t)\mathbf{z}_0$ with respect to the stationary field $h_0\mathbf{z}_0$. However, it is also possible to introduce the time-dependent transversal component $\delta\mathbf{h}\perp(t)$ and examine its dynamic interaction with the superconducting system in Eq. (5). This component generates triplet correlations, but these do not contribute to the order parameter since only singlet pairing in (3) is considered. Consequently, in the second-order perturbation theory with respect to $\alpha k_F/\Delta_0$, there is no linear coupling between the field $\delta\mathbf{h}\perp(t)$ and the gap $\delta\Delta(t)$. This outcome is unsurprising since the only true scalar in this regime $(\delta\mathbf{h}_\perp \cdot \mathbf{h}_0)$ is zero.

IV. EVOLUTION OF QP STATES IN STRONG ZEEMAN FIELD

In this section we address the case of a linearly growing spin-splitting field $h(t) = \gamma t$, which can exceed the equilibrium value of the superconducting gap $\Delta_{\rm eq} \equiv \Delta_0$ and thus provide the crossing of the two QP spectral branches $E_{\uparrow+}(\xi_k)$ and $E_{\downarrow-}(\xi_k)$ from different spin subbands [Figs. 3(a) and 3(c)]. In the collisionless regime and in the absence of RSOC the intersecting spectral branches do not interact, so that the occupation of the quasiparticle states defined at $t = 0$ does not change in time. This means that the self-consistent gap function will not change even above the paramagnetic limit

$h(t) > \Delta_0$ and will be defined by the initial condition $\Delta(t) = \Delta_0$. It is clear from general considerations that the spin-orbit coupling provoke transitions and the interplay between QP states with different spins, and our goal is to investigate the distinctive features of such an interaction and its effect on the superconducting order parameter $\Delta(t)$. As mentioned in Sec. II, we will treat the RSOC energy as a small parameter $\alpha k_F/\Delta \ll 1$. Therefore, we neglect the dependence of the equilibrium gap $\Delta_{\rm eq}$ on α and assume $\Delta_{\rm eq} \equiv \Delta_0$.

A. Adiabatic evolution of QP states

The evolution of QP wave function of the TDBdG equations (1) can be regarded with the help of general adiabatic ansatz

$$\check{\psi}_k(t) = \sum_n C_{kn}(t)\check{\Psi}_{kn}(t), \tag{28}$$

where $\check{\Psi}_{kn}(t)$ are the instantaneous eigenstates of the Hamiltonian (2). Here all negative and positive energy terms with the indices $n = \{\uparrow +, \downarrow +, \uparrow -, \downarrow -\}$ are taken into account. The coefficients $C_{kn}(t)$ define the occupation of QP states and its temporal evolution [similarly to the ansatz (7) used in the previous section]. The initial conditions for $C(t)$ are fixed by the equilibrium distribution at $t = 0$ and have been discussed in Sec. III [see Eq. (10)]. Using short notations two possible initial conditions read as $C_{kn}(t = 0) = \delta_{n,l}$, where $\delta_{n,n'}$ is Kronecker delta and $l = \{\uparrow -, \downarrow -\}$. Thus, for the given l we have $C_{kl}(t = 0) = 1$ and $C_{k(n\neq l)}(t = 0) = 0$.

We introduce the vector

$$\hat{C}_k(t) = (C_{k\uparrow+}, C_{k\downarrow+}, C_{k\uparrow-}, C_{k\downarrow-})^T, \tag{29}$$

which contains all the information about the dynamics of the QP states. Corresponding adiabatic temporal evolution can be described with the help of the unitary operator $\hat{C}_k(t_2) = \hat{U}_k(t_2, t_1)\hat{C}_k(t_1)$ where $\hat{U}_k = \mathrm{diag}(U_{k\uparrow+}, U_{k\downarrow+}, U_{k\uparrow-}, U_{k\downarrow-})$ and

$$U_{kn}(t_2, t_1) = \exp\left(-i\int_{t_1}^{t_2} E_{kn}(t)dt\right). \tag{30}$$

The interaction of the branches $E_{k\uparrow+}(t)$ and $E_{k\downarrow-}(t)$ leads to *avoided crossing* of the QP levels at fixed energy ξ_k with the splitting proportional to αk_F. Thus, the adiabatic approximation is justified only for the levels with $E_k(t) \gg \alpha k_F$, e.g., far enough from the crossing points. Therefore, for the Zeeman field $h(t) \lesssim \Delta_0$ all nonadiabatic transitions are suppressed and the gap function defined by the self-consistency equation (3) is equal to the equilibrium value $\Delta(t) = \Delta_0$.

B. Transition evolution matrix

The avoided crossing between the spectral terms at $h(t) \gtrsim \Delta_0$ should be described in terms of nonadiabatic dynamics. For this we consider the branch intersection as consecutive avoided crossing of pairs of the QP states with fixed energy ξ_k at the time instant $t_0(\xi_k) = \sqrt{\xi_k^2 + \Delta^2}/\gamma$ (Fig. 3). For each crossing at $\xi_k \in (-\omega_D, \omega_D)$ it is possible to formulate the time-dependent Landau-Zener-Stückelberg-Majorana (LZSM) problem [36], which describes the transitions between two QP states with different spins during their temporal evolution. Note that resulting nonadiabatic tunneling is equivalent to dynamical spin-flip process.

In general, the description of such a tunneling (or LZSM problem) requires joint solution of TDBdG equation (1) and self-consistency equation (3). However, some important results can be obtained analytically using certain approximations:

(i) If the time variation of the gap function $\Delta(t)$ is small on the typical tunneling timescale $\tau_{\rm LZ}$ (see Appendix D), then the tunneling of QP states is not affected by the order parameter dynamics.

(ii) The gap $\Delta(t)$ is defined by all states in range $\xi_k \in (-\omega_D, \omega_D)$, and a time-dependent perturbation of the states caused by the dynamical LZSM transition makes a small contribution to the sum over all ξ_k.

Thus, one can neglect the transient dynamics of the coefficients $\hat{C}_k(t)$ in the vicinity of a transition point for each ξ_kth mode. This also means that one can investigate the tunneling problem with the help of so-called transition evolution matrix [36] connecting two adiabatic regimes before ($t < t_0-$) and after ($t > t_0+$) avoided crossing [Fig. 3(e)]. These conditions allow one to effectively decouple the LZSM problem from the self-consistency equation and solve them independently.

Taking into account all these assumptions, the time evolution of the vector $\hat{C}_k(t)$ from the adiabatic ansatz (28) is described as

$$\hat{C}_k(t) = \begin{cases} \hat{U}_k(t, t_0+)\hat{S}_{\rm LZ}\hat{U}_k(t_0-, 0)\hat{C}_k(0), & t > t_0(\xi_k) \\ \hat{U}_k(t, 0)\hat{C}_k(0), & t < t_0(\xi_k). \end{cases} \tag{31}$$

Here the nonadiabatic transitions between QP states are included into transition matrix $\hat{S}_{\rm LZ}$, which acts on the state vector $\hat{C}_k(t)$ at the time instant $t = t_0(\xi_k)$. The matrix $\hat{S}_{\rm LZ}$ can be obtained by considering the interaction of two intersecting energy branches $E_{\uparrow+}$ and $E_{\downarrow-}$ in the TDBdG equation (1). Using so-called diabatic basis [basis of Hamiltonian (2) in the absence of RSOC] one gets a system of dynamical equations, the asymptotic solution of which forms a transition matrix describing the passage through the avoided intersection point. Then we go to the original adiabatic basis (28) and get the matrix $\hat{S}_{\rm LZ}$. The complete derivation of $\hat{S}_{\rm LZ}$ is presented in Appendix D and it reads as

$$\hat{S}_{\rm LZ} = \begin{pmatrix} \sqrt{p_k} & 0 & 0 & \sqrt{1-p_k}e^{i(\dots)} \\ 0 & 1 & 0 & 0 \\ 0 & 0 & 1 & 0 \\ -\sqrt{1-p_k}e^{-i(\dots)} & 0 & 0 & \sqrt{p_k} \end{pmatrix}, \tag{32}$$

where $(\dots) = \chi_k - \theta_k - \frac{\pi}{2}\mathrm{sgn}(\alpha)$. The coefficient

$$p_k = \exp\left[-\delta_{\rm LZ}\frac{\Delta^2}{\xi_k^2 + \Delta^2}\right]$$

is expressed through the dimensionless LZSM parameter $\delta_{\rm LZ} = \pi\alpha^2 k_F^2/\gamma$ and determines the probability of tunneling between QP states with different spins. The transition is accompanied by the appearance of the Stokes phase χ_k (see Appendix D) and the phase $\theta_k = \arg(k_x + ik_y)$.

To avoid confusion, we use the same notations for the spectral branches (4) before ($t < t_0-$) and after ($t > t_0+$) QP transitions, as shown in Fig. 3. Thereby, we do not need to keep track of the indices of the eigenvectors $\check{\Psi}_{kn}(t)$ and the evolution operators $U_{kn}(t)$ from (30). It is sufficient that these functions take into account the permutation of the branches of the spectrum (4), so that all QP levels change their indices after the transition in accordance with the chosen notation.

C. Time dependence of superconducting gap

The time-dependent order parameter subjected to the field $h(t) \gtrsim \Delta_0$ depends on both the adiabatic wave function (28) and nonadiabatic LZSM tunneling (31). The calculation of $\Delta(t)$ can be accomplished using the self-consistent equation (3), which gets the form

$$\Delta(t) = -\frac{\lambda}{2}\sum_l \sum_k \sum_{n,n'} C^*_{kn}(t) C_{kn'}(t) \check{\Psi}^\dagger_{kn} \check{\tau}_\Delta \check{\Psi}_{kn'}, \tag{33}$$

where index l means different initial configurations of the occupation of the QP spectrum at $t = 0$ (see Sec. IV A). The first configuration with $C_{kn}(t=0) = \delta_{n,\uparrow-}$ corresponds to occupation of all QP states belonging to the spectral branch $E_{k,\uparrow-}$ for all momenta with $\xi_k \in (-\omega_D, \omega_D)$. The evolution of the coefficients $C_{kn}(t)$ is determined by Eq. (31) together with Eqs. (29) and (30). Since the branch $E_{k,\uparrow-}$ does not cross with other branches, the coefficients $C_{kn}(t)$ have a trivial adiabatic dynamics, which can be written as

$$\hat{C}_k(t) = \begin{pmatrix} 0 \\ 0 \\ U_{\uparrow-}(t,0) \\ 0 \end{pmatrix}. \tag{34}$$

The second initial configuration with $C_{kn}(t=0) = \delta_{n,\downarrow-}$ leads to the intersection of the filled branch $E_{k,\downarrow-}$ and empty branch $E_{k,\uparrow+}$. Using Eq. (31) we obtain a nontrivial dynamics of the states with LZSM tunneling, which reads as

$$\hat{C}_k(t) = \begin{pmatrix} \sqrt{1-p_k}e^{i(\dots)}U_{\uparrow+}(t,t_0+)U_{\downarrow-}(t_0-,0)\Theta[t-t_0] \\ 0 \\ 0 \\ (\sqrt{p_k}\Theta[t-t_0] + \Theta[t_0-t])U_{\downarrow-}(t,0) \end{pmatrix}. \tag{35}$$

Here $(\dots) = \chi_k - \theta_k - \frac{\pi}{2}\mathrm{sgn}(\alpha)$ and $\Theta(t)$ is the Heaviside function.

Substituting coefficients (34) and (35) obtained from different initial conditions together with the QP wave functions $\hat{\Psi}_{kn}$ from (A3) into the self-consistency equation (33) we get

$$\begin{aligned}\Delta(t) = \lambda &\sum_{|\xi_k| > \sqrt{h^2-\Delta^2}} u_0 v_0 \\ &+ \lambda \sum_{|\xi_k| < \sqrt{h^2-\Delta^2}} \Bigg[\Big(\overbrace{|C_{k\uparrow-}|^2}^{=1} + \overbrace{|C_{k\downarrow-}|^2}^{\propto p_k} - \overbrace{|C_{k\uparrow+}|^2}^{\propto 1-p_k} \Big) \frac{u_0 v_0}{2} \\ &+ u_0 u_1 i e^{-i\theta_k} C^*_{k\uparrow+} C_{k\downarrow-} + v_0 v_1 (-i) e^{i\theta_k} C^*_{k\downarrow-} C_{k\uparrow+} \Bigg].\end{aligned} \tag{36}$$

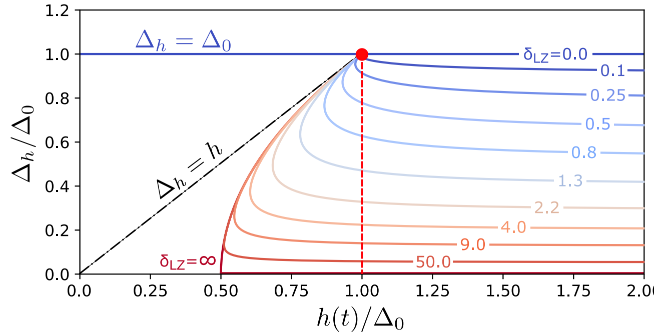

FIG. 4. Quasistatic dependence of the superconducting gap Δ_h on the spin-splitting field $h(t)$ for different values of δ_{LZ} [Eq. (38)]. The dashed-dotted line separates two regions where $\Delta_h \lessgtr h$. The dashed line shows the critical value of the field $h(t) = \Delta_0$ and the red circle marks the point of change in the behavior of the gap Δ_h in the region $\Delta_h > h$. After this point the equilibrium solution $\Delta_h = \Delta_0$ should jump to one of the solutions fixed by the parameter δ_{LZ}.

The last two terms are of the order of $O(\alpha k_F/\Delta)$, so it is convenient to write the gap function as

$$\Delta(t) = \Delta_h[h(t)] + \delta\Delta(t). \tag{37}$$

We have identified two contributions that have significantly different origins: Δ_h is defined by the amplitude of the LZSM tunneling and depends on time only through the Zeeman field $h(t)$; $\delta\Delta(t) \propto O(\alpha k_F/\Delta)$ is defined by cross terms and reflects interference effects between QP wave functions caused by LZSM transitions and depends on time explicitly.

If one neglects the small perturbation $\delta\Delta(t)$ in (37) then it becomes possible to get a simplified self-consistency equation for $\Delta_h[h(t)]$ from Eq. (36). In an implicit form this equation reads as

$$\Delta_h = \Delta_0 \exp\left(\int_1^{h/\Delta_h} \frac{e^{-\delta_{LZ}/s^2} - 1}{\sqrt{s^2-1}} ds \right), \tag{38}$$

where $\delta_{LZ} = \pi\alpha^2 k_F^2/\gamma$ and its numerical integration is shown in Fig. 4. The quasistatic superconducting gap Δ_h behaves differently at $h(t) > \Delta_0$ depending on the regime by which the condensate was driven out of equilibrium.

(i) The value $\delta_{LZ} = 0$ means zero RSOC ($\alpha = 0$), so there is no interaction of the QP states at the intersection of the spectral branches and the trivial solution for the gap $\Delta_h = \Delta_0$ holds.

(ii) The limit of $\delta_{LZ} \ll 1$ with $\gamma \gtrsim \alpha^2 k_F^2$ corresponds to sudden (quench) regime. The spectral branches intersect nonadiabatically, or so rapidly that they do not feel the RSOC. The Landau-Zener tunneling is suppressed and the gap has a weak dependence on the Zeeman field at $h(t) > \Delta_0$:

$$\Delta_h \approx \Delta_0 \exp\left(-\delta_{LZ} \frac{\sqrt{h^2(t) - \Delta_h^2}}{h(t)} \right).$$

(iii) In the opposite limit of $\delta_{LZ} \gg 1$ with $\gamma \ll \alpha^2 k_F^2$ the QPs undergo strong spin-flip tunneling during a slow (almost adiabatic) avoided crossing. This leads to the effective formation of the triplet superconducting correlations (or related triplet component of the anomalous Green function [42]) even for the small RSOC energy $\alpha k_F/\Delta \ll 1$. Such dynamically generated correlations are determined by the rate of field change γ and their effect on the gap can significantly exceed the static mixing of singlet-triplet pairs for $\alpha \neq 0$ [33]. As a result, the singlet gap function (3) is suppressed and the self-consistency equation reads as

$$\Delta_h \approx \begin{cases} \sqrt{\Delta_0(2h(t)-\Delta_0)} \quad \text{for } \Delta_h > h/\delta_{\rm LZ}, \\ \Delta_0 \exp\left(-\delta_{\rm LZ}\frac{\sqrt{h^2(t)-\Delta_h^2}}{h(t)}\right)\frac{\exp(\sqrt{\delta_{\rm LZ}}\sqrt{\delta_{\rm LZ}-1})}{\sqrt{\delta_{\rm LZ}}+\sqrt{\delta_{\rm LZ}-1}} \\ \quad \text{for } \Delta_h < h/\delta_{\rm LZ}. \end{cases}$$

However, the appearance of these triplet correlations does not result in the generation of the spin-triplet pairing order parameter since within our model we do not introduce any nonzero coupling constant for the triplet pairing channel [43].

(iv) The critical value $\delta_{\rm LZ} \to \infty$ corresponds to the complete Landau-Zener spin-flip tunneling, so that there are no QPs at the energies $E > 0$. In this case we have restored the thermodynamically metastable branch $\Delta_h \approx \sqrt{\Delta_0(2h(t)-\Delta_0)}$ from well-known static case [31].

The actual behavior of the gap in time must be determined by switching between different branches of $\Delta_h[h]$ as the Zeeman field $h(t)$ increases. The first solution, which is fixed by the initial condition $\Delta_h(t=0)=\Delta_0$, holds until $h(t)=\Delta_0$, where Δ_h goes to another unique possible solution $\Delta_h[h]$ for a given $\delta_{\rm LZ}$ (see the red point and black dashed line in Fig. 4). The question of the exact dynamics of the gap in the jump region is difficult because, due to the rapid change in the Δ_h, the decoupling of the LZSM problem and self-consistency equation may not be guaranteed (Sec. IV B). It is qualitatively expected that the jump at $t \approx \Delta_0/\gamma$ should be smeared both by nonzero static contribution of SOC to the gap (since the equilibrium gap value depends on α) and by the QP tunneling dynamics. At large times $h(t) \gg \Delta_0$ there are no transitions between the QP states ($p_k \to 1$) since the splitting between the spectral branches becomes zero and therefore the gap tends to the constant asymptotics $\Delta_h(\infty)$.

D. QP interference effects

In addition to the quasistatic term Δ_h, the gap equation (36) also contains small rapidly oscillating term

$$\delta\Delta(t) = \lambda \sum_{|\xi_k|<\sqrt{h^2-\Delta^2}} u_0u_1 ie^{-i\theta}C^*_{k\uparrow+}C_{k\downarrow-} + v_0v_1(-i)e^{i\theta}C^*_{k\downarrow-}C_{k\uparrow+}, \tag{39}$$

arising from the interference of the QP states which have experienced LZSM transitions. It is obvious that in its structure this function resembles the collective Higgs mode, which is excited in a natural way during the redistribution of states in the QP spectrum. Let us look at it in more details. Using the time-dependent coefficients (34) and (35) we obtain

$$\frac{\delta\Delta(t)}{\lambda N(0)} = \int_{-\sqrt{h^2-\Delta^2}}^{\sqrt{h^2-\Delta^2}} \sqrt{p_k}\sqrt{1-p_k}G(\xi,t)\cos[D_k(t)]d\xi, \tag{40}$$

where we introduce the dynamical phase $D_k(t) = 2\int_{t_0}^t [E_0 - h(t)]dt + \chi_k + \pi$ and the function $G(\xi,t) = \text{sgn}(\alpha)(u_0u_1 + v_0v_1)$. The function $G(\xi)$ is proportional to $\alpha k_F/\Delta$, which means that $\delta\Delta(t)$ is parametrically small and can be considered against the background of the main change in the gap Δ_h from Eq. (38).

For the integral (40), it is easy to estimate the asymptotic behavior at large times $\Delta_0/\gamma \ll t$. The dynamical phase is written as $D_k(t) = -(E_0^2+\gamma^2t^2)/\gamma + \chi_k + \pi + 2E_0t$ for the spin-splitting field $h(t)=\gamma t$. Here $2E_0t$ is a fast oscillating term at $t\to\infty$ and one can use a stationary phase approximation for the ξ integration in Eq. (40) with the stationary phase point $\xi = 0$. Using Eq. (A6) for $G(\xi=0,t)$, we find the asymptotic behavior of $\delta\Delta(t)$:

$$\delta\Delta(t) \approx \lambda N(0)e^{-\delta_{\rm LZ}/2}\sqrt{1-e^{-\delta_{\rm LZ}}}\frac{|\alpha|k_F}{2(\gamma t-\Delta_h)} \times \sqrt{\frac{\pi\Delta_h}{t}}\cos\left(\frac{(\gamma t-\Delta_h)^2}{\gamma}+\frac{3\pi}{4}-\chi_0\right), \tag{41}$$

where $\Delta_h[h(t\to\infty)]$ from Eq. (38) is a constant determined by $\delta_{\rm LZ}$. The result obtained means that the collective interference between the two QP states at each ξ_k after LZSM crossing behaves at large times as a modified Higgs mode. Due to linear dependence $h(t)$, this mode has a modulated frequency and polynomial damping law $\propto t^{-3/2}$ arising from the inhomogeneous broadening of the mode. Note that for large times only the contribution from the point $\xi = 0$ survives, so the amplitude of $\delta\Delta(t)$ does not depend on the number of redistributed states in the QP spectrum.

If the linear growth of the spin-splitting field $h(t)$ stops at a certain value $h_f > \Delta_0$ after the redistribution of some of the QP states, then the accumulated dynamic phase $D_k(t)$ and the gap fluctuation will depend only on this value h_f:

$$\delta\Delta(t) \approx \lambda N(0)e^{-\delta_{\rm LZ}/2}\sqrt{1-e^{-\delta_{\rm LZ}}}\frac{|\alpha|k_F}{2(h_f-\Delta_h)}\sqrt{\frac{\pi\Delta_h}{t}} \times \cos\left(2(h_f-\Delta_h)t-\frac{3\pi}{4}-\frac{\Delta_h^2-h_f^2}{\gamma}+\chi_0\right). \tag{42}$$

The specific spectral distortion occurring between two branches $E_{k\uparrow+}$ and $E_{k\downarrow-}$ during the Landau-Zener dynamics at $h(t) < h_f$ acts as an initial perturbation for the gap function at $t = h_f/\gamma$. The free gap dynamics at $t > h_f/\gamma$ resembles the Higgs mode with $\delta\Delta(t) \propto \cos[2(h_f-\Delta_h)t]/\sqrt{t}$ at the frequency $\omega = 2|\Delta_h - h_f|$ (or $\omega = \omega_-$ in our previous notations) with the standard damping law. It is interesting that the amplitude of this mode proportional to $|\alpha|k_F$ instead of $\alpha^2k_F^2$ as it is expected in the case of small perturbations (Sec. III). Such amplification is a direct consequence of the intersection of two specific spectral branches and the subsequent nonadiabatic dynamics. Thus, this mode turns out to be leading in comparison with other nonadiabatic corrections arising due to the interaction of all QP spectral branches. Note that the method for calculating the self-consistency equation developed in Sec. III can be combined with the Landau-Zener problem (D3) and all corrections can be computed within the perturbation theory.

E. Density of states and distribution function

Rearrangement of the spectrum as a result of the intersection of spectral branches naturally leads to a change of the structure of the density of states (DOS), that has become time dependent. Since the temporal evolution of the spectrum is adiabatic except the small region where the crossing occurs one can use the quasistatic description of the DOS. For the small RSOC the DOS for one spin projection can be written in terms of Bogoliubov–de Gennes functions

$$N_\uparrow(E,t) \approx \sum_k \sum_{n=\uparrow+,\uparrow-} |u_0|^2\delta(E-E_{kn}) + |v_0|^2\delta(E+E_{kn}). \quad (43)$$

Here we use static QP amplitudes u_0 and v_0 [see Eq. (A4)] to distinguish the particle and hole contributions and $E_{k\uparrow\pm}$ are defined in Eq. (4). The calculation of $N_\uparrow$ is cumbersome because the RSOC shifts the spectral branches and opens a minigap $\propto \alpha k_F$ at $E=0$ (Appendix E). For the small RSOC parameter these changes are negligible and one can use a standard expression for the DOS

$$\frac{N_\uparrow(E,t)}{N(0)} \approx \frac{|E+h(t)|}{\sqrt{(E+h(t))^2-\Delta_h^2}}. \quad (44)$$

Here the gap function Δ_h is taken from (38) and two coherence peaks are present at $E=\pm\Delta_h - h(t)$.

The amplitude of the QP wave function $\psi_k(t)$ from (28) contains the information about filling (or occupation) of the ξ_kth state. More precisely, the coefficients $|C_{k\uparrow\pm}(t)|^2$ and $|C_{k\downarrow\pm}(t)|^2$ can serve as an effective distribution functions $f_{\uparrow\downarrow}(E)$ for QPs with different spin projections. As discussed in Sec. IV C, the temporal evolution of these coefficients is determined by the LZSM problem, and for spin-up states one has

$$|C_{k\uparrow-}(t)|^2 = 1,$$
$$|C_{k\uparrow+}(t)|^2 = (1-p_k)\Theta\left[\sqrt{h^2(t)-\Delta_h^2}-\xi_k\right],$$

which can be rewritten as a distribution function

$$f_\uparrow(E,t) \approx \begin{cases} 0, & E>0 \\ 1-\exp\left[-\frac{\delta_{\rm LZ}\Delta_h^2}{(E+h(t))^2}\right], & \Delta_h - h < E < 0 \\ 1, & E < \Delta_h - h. \end{cases} \quad (45)$$

The dependence $f_\uparrow(E)$ is shown in Fig. 4 for $\delta_{\rm LZ}=0.5$. The most pronounced change of the distribution function occurs at $E\approx \Delta_h - h$ since for large QP energies the LZSM tunneling is suppressed. For the opposite spin projection the DOS $N_\downarrow(E)$ has the similar structure (44) with $h\to -h$, while the corresponding distribution function $f_\downarrow(E)$ is different and is given by Eqs. (34) and (35). The DOS structure and effective distribution function enable the calculation of a system's optical or transport response, which can be experimentally measured.

F. Dynamical magnetization of QP gas

Nonadiabatic LZSM tunneling of QP states causes a spin imbalance in the spectrum, which results in the appearance of nonzero dynamical magnetization. Using (28) we can write an expression for the z component of the magnetization per unit volume

$$m_z(t) = \mu_B \sum_{\rm i.c.} \check\psi_k^\dagger(t)\check\tau_m\check\psi_k(t), \quad (46)$$

where $\check\tau_m = (\hat\tau_0+\hat\tau_z)\otimes\hat\sigma_z/2$; the vector $\check\psi_k(t)$ is a solution of the TDBdG problem (28) and "i.c." means the summation over all initial conditions [see Eq. (3)]. Due to symmetry and homogeneity of the problem for the field $\mathbf{h}(t)=h(t)\mathbf{z}_0$ the transversal components of the magnetization $m_{x,y}(t)$ are zero.

Taking the dynamical amplitudes $C_n(t)$ from (34) and (35) and implementing the same procedure as for the self-consistency equations (36) and (37) we found that the magnetization can be written as

$$m_z(t) = m_h[h(t)] + \delta m(t). \quad (47)$$

As in the case of the gap equation (37) we have two contributions: m_h which is a quasistatic function of $h(t)$ arising from the redistribution of the quaiparticle states, and $\delta m(t)\propto \alpha k_F$ which is small oscillatory term originated from the interference of the redistributed states. The first term can be easily calculated with the help of the quasiparticle density

$$n_\sigma(t) = \int N_\sigma(E,t) f_\sigma(E,t)dE, \quad (48)$$

where $\sigma=\{\uparrow,\downarrow\}$. Corresponding spin imbalance results in the dynamical magnetization $m_h=\mu_B(n_\uparrow - n_\downarrow)$, which is shown in Fig. 5(a).

For $h(t)<\Delta_0$ there is no crossing of the QP spectral branches and according to our model there is no tunneling between QP states, therefore, $m_h=0$. Once the intersection has occurred at $h(t)=\Delta_0$, the distribution functions $f_{\uparrow,\downarrow}(E)$ transform and nonzero spin imbalance $n_\uparrow - n_\downarrow$ is generated. Due to the jump of Δ_h function at $h(t)=\Delta_0$ (Fig. 4) the magnetization m_h at this point also has a jump discontinuity. At large times the tunneling of QP states is suppressed, therefore, the magnetization is saturated to a constant value determined

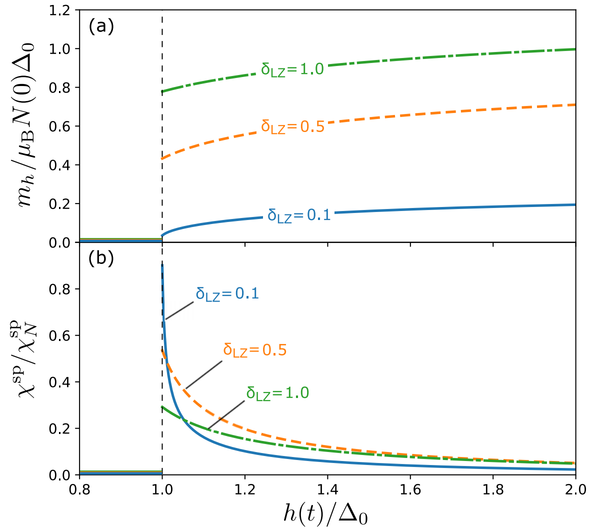

FIG. 5. (a) Dynamical magnetization m_h per unit volume induced by the nonadiabatic tunneling of QP states and (b) corresponding spin susceptibility $\chi^{\rm sp}$ versus time-dependent spin-splitting field $h(t)$ for different values of $\delta_{\rm LZ}$.

by the parameter $\delta_{\rm LZ}$. Obviously, an increase in $\delta_{\rm LZ}$ makes the spin-flip tunneling more efficient and thereby increases the maximum value of m_h. The second term in (47) resembles the Higgs mode term (39) and gives negligible contribution to $m_z(t)$, therefore, it can be discarded.

In addition, one can compute the dynamical susceptibility of the QP gas in the Zeeman field of the general form $h(t) = \mu_{\rm B} H(t)$. It is known that an orbital and a spin part of the magnetic susceptibility can be splitted in the case of small spin-orbital effects [42]. Since we consider a homogeneous system and neglect all orbitals effects only the spin part plays a role, which can be written as

$$\chi^{\rm sp}[h(t)] = \mu_B \frac{\partial m_h}{\partial h}. \tag{49}$$

The ratio of the numerically calculated susceptibility $\chi^{\rm sp}[h(t)]$ and the normal susceptibility $\chi^{\rm sp}_N = 2\mu_B^2 N(0)$ [44] is shown if Fig. 5(b). It is seen that spin-flip tunneling in the QP spectrum provokes a paramagnetic response of the superconducting condensate. The function (49) should have a singularity $\chi^{\rm sp} \propto [h(t) - \Delta_0]^{-1/2}$ in the vicinity of $h(t) \approx \Delta_0$, which is defined by the shape of the QP spectrum at $k \approx k_F$ and has the same origin as the coherence peak in the DOS (44). However, due to the jump of the order parameter Δ_h at this point we observe shifted peaks, which have to be smeared out near $h(t) = \Delta_0$ if more realistic model of LZSM tunneling (Sec. IV B) is taken into account. We note again that we discuss only the dynamic contribution to the susceptibility, which, generally speaking, has to be added to the static one, which is not equal to zero at $T = 0$ in the presence of SOC [42,44].

V. EXPERIMENTAL PERSPECTIVES

As an experimental platform for detecting the described effects, we propose to use S/F hybrid structures. The ferromagnetic layer can serve as a source of both Rashba spin-orbit coupling and an exchange field. Since it is important to remove orbital effects from the system, the most suitable geometry for superconductor is either a thin film or an one-dimensional nanowire [45]. For the small layer thicknesses, the exchange interaction can be averaged in the direction perpendicular to the layers, giving a homogeneous effective exchange field inside the superconductor.

The excitation of spin-split Higgs modes in superconductors requires frequencies of the order of $\Delta_0/\hbar$, which vary from the far infrared to the terahertz range. The laser excitation of modes seems to be the most practical and feasible, and their detection can be implemented using the ultrafast pump-probe spectroscopy [10–12].

We propose two possible ways to generate rapidly changing modulus of the spin-splitting field $h(t)$:

(i) If the S/F bilayer possesses a strongly anisotropic exchange, so that the Zeeman energy $\propto \mathbf{M}_F \hat{g} \boldsymbol{\sigma}$ in Eq. (6) is defined through the tensorial g factor, then the absolute value of the exchange field is no more determined only by the absolute value of the magnetic moment $|\mathbf{M}_F(t)| = \text{const}$. Thus, we can get a pronounced component of the spin-splitting field $h_z(t)$ varying in time just for a standard precession of $\mathbf{M}_F(t)$. Such approach can be reasonable amid a progress in the ultrafast optical control of magnetization in various materials [23,46–48].

(ii) Another possibility is based on the obvious fact that the field $\mathbf{h}$ is determined not only by the magnetic moment,but also by the penetration length of the wave functions of electrons from superconductor to the insulator. This penetration clearly depends on the potential jump at the S/F interface and, thus, can be tuned by the electric field effect. Certainly, to realize a noticeable field effect we need to take a ferromagnetic film with a rather narrow energy gap in the band spectrum, e.g., a film of ferromagnetic semiconductor. In this case the exchange field value can be modulated by simply applying a time-dependent gate potential to the semiconducting layer.

Finally, we present parameter estimates for the experimental observation of LZSM transitions in the QP spectrum. For example, consider $\Delta_0 = 0.1$ meV (for $T_c \approx 1$ K) and $\alpha k_F \sim 10^{-3}$ meV $\ll \Delta_0$. Then the constraint for the small tunneling rate is $\hbar\gamma \gtrsim \alpha^2 k_F^2$ in dimensional units, which is equivalent to $\gamma \gtrsim 10^{-3}$ meV/ns. Consider inelastic relaxation of QP with a typical time $\tau_{\rm ph} \sim 100$ ns in the case of the electron-phonon scattering at low temperatures [49,50]. The collisionless regime is maintained at $t \ll \tau_{\rm ph}$, which corresponds to times $t \lesssim 10$ ns. Under such conditions the field $h(t) = \gamma t \sim \Delta_0$ is achievable only for $\gamma \sim 10^{-2}$ meV/ns.

VI. CONCLUSIONS

To sum up, we analyzed the coherent dynamics of the superconducting condensate in the presence of Zeeman field and SOC in collisionless regime. First, it was established that the Higgs mode of the superconducting gap is sensitive to the spin-splitting field h_0 and can be directly triggered by either its harmonic perturbation $\delta h(t)$ or by a nonadiabatic quench induced by a laser pulse. Second, it was shown that the field $h(t) \sim t$ can provoke an avoided crossing of the QP spectral branches accompanied by adiabatic spin-flip tunneling of the QPs between the different branches. Corresponding redistribution of the QPs in the spectrum leads to the appearance of the dependence $\Delta[h(t)]$ and generation of the interference effects. Emerging spin imbalance reveals itself in the effective dynamical distribution function and in a generation of a weak magnetization of the QP gas. We consider S/F structures to be good candidates for experimental realization of the described findings.

ACKNOWLEDGMENTS

This work has been supported by ANR SUPERFAST, the LIGHT S&T Graduate Program, and the Russian Science Foundation (Grant No. 21-72-10161) in part of the study of dynamics in strong Zeeman field. The study of the linearized gap dynamics was supported by Center of Excellence "Center of Photonics" funded by The Ministry of Science and Higher Education of the Russian Federation, Contract No. 075-15-2022-316.

APPENDIX A: EIGENVECTORS

The instantaneous eigenvectors of the Hamiltonian $\check{\mathcal{H}}(k,t)$ from Eq. (2) can be written as

$$\check{\Psi}_{kn}(t) = \frac{1}{\sqrt{1 + a_{1n}^2 + a_{2n}^2 + a_{3n}^2}} \begin{pmatrix} 1 \\ -ia_{1n}e^{i\theta_k} \\ -ia_{2n}e^{i\theta_k} \\ a_{3n} \end{pmatrix}, \tag{A1}$$

where we have defined the phase $\theta_k = \arg(k_x + ik_y)$ and real coefficients

$$a_{1n} = \frac{(h+E_{kn})^2 - E_0^2 - \alpha^2 k^2}{2\alpha k(\xi_k + h)},$$
$$a_{2n} = \frac{\alpha k}{\Delta} - \frac{E_{kn} - \xi_k - h}{\Delta} a_{1n},$$
$$a_{3n} = \frac{E_{kn} - \xi_k + h}{\Delta} - \frac{\alpha k}{\Delta} a_{1n}. \tag{A2}$$

The instantaneous eigenvalues of $\check{\mathcal{H}}(k,t)$ are

$$E_{kn}(t) \equiv E_{k\sigma\pm}(t) = \pm\sqrt{E_0^2 + \alpha^2 k^2 + h^2(t) \mp \mathrm{sgn}(\sigma) 2\sqrt{\xi_k^2\alpha^2 k^2 + h^2(t)E_0^2}},$$

where $E_0 = \sqrt{\xi_k^2 + \Delta^2}$; the subscript $\pm$ refers to spectral branch above and below the Fermi level and $\sigma = \{\uparrow, \downarrow\}$ denotes a spin subband. Note that the Hamiltonian (2) implies the symmetry relations between the energies $E_{k\uparrow+} = -E_{k\downarrow-}$ and $E_{k\downarrow+} = -E_{k\uparrow-}$, and between the corresponding eigenvectors $\check{\Psi}_{k\uparrow+} = i\hat{\tau}_y \otimes \hat{\sigma}_z \check{\Psi}^*_{k\downarrow-}$ and $\check{\Psi}_{k\downarrow+} = i\hat{\tau}_y \otimes \hat{\sigma}_z \check{\Psi}^*_{k\uparrow-}$, where $\hat{\tau}_i(\hat{\sigma}_i)$ is the Pauli matrix in the Nambu (spin) space.

For the case of weak SOC $\alpha k_F \ll \{E_F, h(t), \Delta(t)\}$ the eigenvectors (A1) can be expanded up to the first order in $\alpha k_F/\Delta$ as follows:

$$\check{\Psi}_{k\uparrow+} \approx \begin{pmatrix} u_0 \\ -iu_1 e^{i\theta_k} \\ -iv_1 e^{i\theta_k} \\ v_0 \end{pmatrix}, \quad \check{\Psi}_{k\downarrow+} \approx \begin{pmatrix} iu_1 e^{-i\theta_k} \\ -u_0 \\ v_0 \\ -iv_1 e^{-i\theta_k} \end{pmatrix},$$
$$\check{\Psi}_{k\uparrow-} \approx \begin{pmatrix} -v_0 \\ iv_1 e^{i\theta_k} \\ -iu_1 e^{i\theta_k} \\ u_0 \end{pmatrix}, \quad \check{\Psi}_{k\downarrow-} \approx \begin{pmatrix} -iv_1 e^{-i\theta_k} \\ v_0 \\ u_0 \\ -iu_1 e^{-i\theta_k} \end{pmatrix}. \tag{A3}$$

Here we define equilibrium QP amplitudes

$$u_0 = \frac{1}{\sqrt{2}}\sqrt{1 + \frac{\xi_k}{E_0}}, \quad v_0 = \frac{1}{\sqrt{2}}\sqrt{1 - \frac{\xi_k}{E_0}}, \tag{A4}$$

and

$$u_1 \approx \alpha k \frac{h - \xi_k}{2h(E_0 - h)} u_0, \quad v_1 \approx \alpha k \frac{(h+\xi_k)(E_0 - \xi_k)}{2h\Delta(E_0 - h)} u_0 \tag{A5}$$

correspond to the triplet component of the QP wave functions.

The function $G(\xi, t) = \mathrm{sgn}(\alpha)(u_0 u_1 + v_0 v_1)$ from Eq. (40) at the stationary phase point $\xi = 0$ can be found from (A4) and (A5) by putting $\Delta \approx \Delta_h$ [see Eq. (38)] and reads as

$$G(0,t) \approx \frac{|\alpha| k_F}{2(h(t) - \Delta_h)}. \tag{A6}$$

APPENDIX B: DERIVATION OF LINEARIZED SELF-CONSISTENCY EQUATION

We start with the linearized (8) and (11) dynamical equations

$$i\frac{\partial}{\partial t}\delta C_{km} = \sum_n \check{\Psi}_m^\dagger \check{\mathcal{V}}(t) \check{\Psi}_n e^{-i(E_n - E_m)t}(\delta_{n,l} + \delta C_{kn}), \tag{B1}$$

where $\delta_{n,n'}$ is Kronecker delta, the indices $n, m = \{\uparrow+, \downarrow+, \uparrow-, \downarrow-\}$ number all QP branches, and $l = \{\uparrow-, \downarrow-\}$ corresponds to two possible initial configurations [see Eq. (10)]. The compact form of the self-consistency equation for the gap (9) is

$$\Delta_{\rm eq} + \delta\Delta(t) = -\frac{\lambda}{2}\sum_l \sum_k \sum_{n,n'} (\delta_{n,l} + \delta C_{kn}(t)^*)(\delta_{n',l} + \delta C_{kn'}(t)) \times e^{-i(E_{n'} - E_n)t} \check{\Psi}^\dagger_{kn} \check{\tau}_\Delta \check{\Psi}_{kn'}. \tag{B2}$$

As was mentioned in Sec. II, we neglect the effect of RSOC on the equilibrium value of the gap, which can be taken as $\Delta_{\rm eq} = \Delta_0$. It also makes sense to omit the negligibly small corrections from the RSOC to the energy spectrum, so one can put $E_n \equiv E_{k\sigma\pm} \approx \pm E_0 - \mathrm{sgn}(\sigma) h_0$.

Equations (B1) and (B2) can be simplified and written as follows:

$$\frac{\partial f_1}{\partial t} = ie^{i[2(E_0 - h_0)t]}[\mathcal{A}\delta\Delta(t) - \mathcal{B}\delta h(t)],$$
$$\frac{\partial f_2}{\partial t} = ie^{i[2(E_0 + h_0)t]}[\mathcal{A}\delta\Delta(t) + \mathcal{B}\delta h(t)],$$
$$\frac{\partial g}{\partial t} = i\frac{\xi}{E_0} e^{i(2E_0 t)}\delta\Delta(t),$$
$$\delta\Delta(t) = \left\langle \frac{\mathcal{A}}{2}\mathrm{Re} f_1(t) e^{-i[2(E_0 - h_0)t]}\right\rangle + \left\langle \frac{\mathcal{A}}{2}\mathrm{Re} f_2(t) e^{-i[2(E_0 + h_0)t]}\right\rangle + \left\langle \frac{\xi}{E_0}\mathrm{Re} g(t) e^{-i(2E_0 t)}\right\rangle. \tag{B3}$$

We have used the notation $\langle \dots \rangle = \lambda \sum_k \approx \lambda N(0)\int_{-\omega_D}^{\omega_D} d\xi$ and introduced new complex-valued functions

$$f_1 \equiv -ie^{i\theta}\delta C_{\uparrow+}, \quad g_1 \equiv -\delta C_{\downarrow+},$$
$$f_2 \equiv -ie^{-i\theta}\delta C_{\downarrow+}, \quad g_2 \equiv -\delta C_{\uparrow+},$$
$$g = \frac{g_1 + g_2}{2}, \tag{B4}$$

where the subscript corresponds to the two possible initial conditions. The functions

$$\mathcal{A}(\xi) = 2(u_0 u_1 + v_0 v_1) \approx \alpha k_F \frac{E_0 h - \xi^2}{E_0 h(E_0 - h)},$$
$$\mathcal{B}(\xi) = 2(u_0 v_1 + u_1 v_0) \approx \alpha k_F \frac{\Delta_0}{E_0(E_0 - h)} \tag{B5}$$

have the lowest order in αk_F parameter (Appendix A) and are even in ξ. All terms odd in ξ in Eq. (B3) are related to the imaginary part of $\delta\Delta(t)$ and vanish due to the approximate electron-hole symmetry of BdG Hamiltonian (2), due to which the density of states is approximated as $N(\xi) \approx N(0)$ in the $\langle \dots \rangle$ integration [51].

Applying the Laplace transform $f(s) = \int_0^\infty e^{-st} f(t) dt$ with $s = i\omega + \zeta$ (where $\zeta \to 0$) for Eq. (B3) we obtain the gap equation in the complex plane, which is found to be

$$\begin{aligned}\delta\Delta(s) &= \delta\Delta(s)\left\langle\frac{2\xi^2}{E_0}\frac{1}{s^2+4E_0^2}\right\rangle + \delta\Delta(s)\left\langle\mathcal{A}^2(\xi)\frac{(E_0+h_0)}{s^2+4(E_0+h_0)^2}\right\rangle + \delta\Delta(s)\left\langle\mathcal{A}^2(\xi)\frac{(E_0-h_0)}{s^2+4(E_0-h_0)^2}\right\rangle \\ &+ \delta h(s)\left\langle\mathcal{A}(\xi)\mathcal{B}(\xi)\frac{(E_0+h_0)}{s^2+4(E_0+h_0)^2}\right\rangle - \delta h(s)\left\langle\mathcal{A}(\xi)\mathcal{B}(\xi)\frac{(E_0-h_0)}{s^2+4(E_0-h_0)^2}\right\rangle \\ &+ \left\langle f_1'(0)\frac{\mathcal{A}(\xi)}{2}\frac{s}{s^2+4(E_0-h_0)^2}\right\rangle + \left\langle f_1''(0)\frac{\mathcal{A}(\xi)(E_0-h_0)}{s^2+4(E_0-h_0)^2}\right\rangle + \left\langle f_2'(0)\frac{\mathcal{A}(\xi)}{2}\frac{s}{s^2+4(E_0+h_0)^2}\right\rangle \\ &+ \left\langle f_2''(0)\frac{\mathcal{A}(\xi)(E_0+h_0)}{s^2+4(E_0+h_0)^2}\right\rangle + \left\langle g'(0)\frac{\xi}{E_0}\frac{s}{s^2+4E_0^2}\right\rangle + \left\langle g''(0)\frac{2\xi}{s^2+4E_0^2}\right\rangle. \end{aligned} \quad \text{(B6)}$$

Here $f = f' + if''$ and the initial conditions $f_{1,2}(0) = f_{1,2}(t=0)$, $g(0) = g(t=0)$ implicitly contain the initial value of the gap perturbation $\delta\Delta(t=0)$. Now we can single out functions of s with different singularities in the complex plane and denote them using short notations

$$\begin{aligned}\mathcal{K}_0(s) &= \left\langle\frac{2\xi^2}{E_0}\frac{1}{s^2+4E_0^2}\right\rangle, \\ \mathcal{K}_\pm(s) &= \left\langle\mathcal{A}^2(\xi)\frac{(E_0\pm h_0)}{s^2+4(E_0\pm h_0)^2}\right\rangle, \\ \mathcal{F}_\pm(s) &= \left\langle\mathcal{A}(\xi)\mathcal{B}(\xi)\frac{(E_0\pm h_0)}{s^2+4(E_0\pm h_0)^2}\right\rangle. \end{aligned} \quad \text{(B7)}$$

Other terms in Eq. (B6) can be grouped into one function

$$\begin{aligned}\mathcal{I}(s) &= \left\langle\frac{\mathcal{A}(\xi)}{2}\frac{sf_1'(0)+2(E_0-h_0)f_1''(0)}{s^2+4(E_0-h_0)^2}\right\rangle \\ &+ \left\langle\frac{\mathcal{A}(\xi)}{2}\frac{sf_2'(0)+2(E_0+h_0)f_2''(0)}{s^2+4(E_0+h_0)^2}\right\rangle \\ &+ \left\langle\frac{\xi}{E_0}\frac{sg'(0)+2E_0g''(0)}{s^2+4E_0^2}\right\rangle, \end{aligned} \quad \text{(B8)}$$

which actually is an *effective* initial condition for the dynamics of the gap $\delta\Delta(t)$ and originated from the initial nonequilibrium perturbations of the QP population $\delta C_{kn}(t=0)$.

The functions $\mathcal{A}$ and $\mathcal{B}$ are of the first order in the small parameter $\alpha k_F/\Delta$, therefore, we have

$$\mathcal{K}_0(s) \propto O\left(\frac{\alpha^0 k_F^0}{\Delta_0^0}\right), \quad \mathcal{K}_\pm(s), \mathcal{F}_\pm(s) \propto O\left(\frac{\alpha^2 k_F^2}{\Delta_0^2}\right).$$

It can be shown that the the difference $[\mathcal{F}_+(s) - \mathcal{F}_-(s)]$ is proportional to h_0. This allows one to write the terms with $\delta h(t)$ in (B6) as $\delta h(s)[\mathcal{F}_+(s) - \mathcal{F}_-(s)]$ or $[\mathbf{h}_0 \cdot \delta\mathbf{h}(s)][\mathcal{F}_+(s) - \mathcal{F}_-(s)]/h_0$, where both vectors are oriented along the $\mathbf{z}_0$ axis. By rewriting Eq. (B6) with the new introduced functions (B7) we get the self-consistency equation (12).

APPENDIX C: LONG-TIME BEHAVIOR OF $\delta\Delta(t)$

The susceptibility $\mathrm{Im}\chi_{\Delta\Delta}(s)|_{\zeta\to 0} = \mathrm{Im}\chi_{\Delta\Delta}(\omega)$ in Eq. (22) has strongly dominant terms in the vicinity of different branch points in the interval $\omega \in [\omega_-, \infty)$. In order to demonstrate this, the function $\mathrm{Im}\chi_{\Delta\Delta}(s)$ can be expanded in a series up to the second order in the parameter $\alpha k_F/\Delta$, and this expansion must be carried out accurately near the branch points and may differ in different regions of ω. Therefore, we assume that the value of the integral is determined by these dominant contributions of $\mathrm{Im}\chi_{\Delta h}(\omega)$ and can be evaluated sequentially as $\int_{\omega_-}^{\infty} = \int_{\omega_-}^{\omega_0} + \int_{\omega_0}^{\omega_+} + \int_{\omega_+}^{\infty}$. Let us consider the small regions $\Omega \ll \omega_{0,\pm}$ in the vicinity of these points separately.

(i) Close to the point $\omega = \omega_- + \Omega$ the term $\mathcal{K}_-''(\omega)$ dominates:

$$\mathcal{K}_-''(\Omega) \approx -\lambda N(0)\frac{\pi\Delta_0\mathcal{A}^2(0)}{4\sqrt{\Delta_0\Omega}} \propto \frac{1}{\sqrt{\Omega}}. \quad \text{(C1)}$$

Despite the kernel $1 - \mathcal{K}_0'(\omega)$ goes to zero at $\omega \to \omega_0$ there is no singularity in $\chi_{\Delta\Delta}(\omega)$ at this point due to the small terms of the order of $(\alpha k_F)^2$ in the denominator. Therefore, the region in the vicinity of ω_0 will not contribute to the integral. Thus, the behavior of the first integral for $\omega \in [\omega_-, \omega_0)$ at large time $h_0 t \gg 1$ can be estimated as

$$\begin{aligned}\int_{\omega_-}^{\omega_0} &\approx \mathrm{Im}\left[\frac{\mathcal{I}_0 e^{i\omega_- t}}{[1-\mathcal{K}_0'(\omega_-)]^2}\int_0^{\omega_0-\omega_-}\mathcal{K}_-''(\Omega)e^{i\Omega t}d\Omega\right] \\ &\approx -\lambda N(0)\frac{\pi^{3/2}\Delta_0\mathcal{A}^2(0)}{4\sqrt{\Delta_0 t}}\frac{\mathrm{Im}[\mathcal{I}_0 e^{i(\omega_- t+\pi/4)}]}{[1-\mathcal{K}_0'(\omega_-)]^2}. \end{aligned} \quad \text{(C2)}$$

(ii) In the vicinity of the branch point $\omega = \omega_0 + \Omega$ the main contribution is defined by

$$\mathcal{K}_0''(\Omega) \approx -\lambda N(0)\frac{\pi}{2\Delta_0}\sqrt{\Delta_0\Omega} \propto \sqrt{\Omega}. \quad \text{(C3)}$$

Thus, at large times $h_0 t \gg 1$ we get

$$\begin{aligned}\int_{\omega_0}^{\omega_+} &= \int_{\omega_0}^{\omega_+}\frac{1}{\mathcal{K}_0''(\omega)}\mathrm{Im}[e^{i\omega t}\mathcal{I}_0]d\omega \\ &\approx -\frac{2\sqrt{\Delta_0}}{\sqrt{\pi t}}\frac{1}{\lambda N(0)}\mathrm{Im}[\mathcal{I}_0 e^{i(\omega_0 t+\pi/4)}]. \end{aligned} \quad \text{(C4)}$$

(iii) For the last branch point $\omega = \omega_+ + \Omega$ the kernel $\mathcal{K}_+''(\omega)$ dominates:

$$\mathcal{K}_+''(\Omega) \approx -\lambda N(0)\frac{\pi\Delta_0\mathcal{A}^2(0)}{4\sqrt{\Delta_0\Omega}} \propto \frac{1}{\sqrt{\Omega}}. \quad \text{(C5)}$$

At large times $h_0 t \gg 1$ we get

$$\begin{aligned}\int_{\omega_+}^{\infty} &\approx \int_{\omega_+}^{\infty}\frac{\mathcal{K}_+''(\omega)\mathrm{Im}[e^{i\omega t}\mathcal{I}_0]}{[1-\mathcal{K}_0'(\omega_+)]^2+[\mathcal{K}_0''(\omega_+)]^2}d\omega \\ &\approx -\lambda N(0)\frac{\pi^{3/2}\Delta_0\mathcal{A}^2(0)}{4\sqrt{\Delta_0 t}}\frac{\mathrm{Im}[\mathcal{I}_0 e^{i(\omega_+ t+\pi/4)}]}{[1-\mathcal{K}_0'(\omega_+)]^2+[\mathcal{K}_0''(\omega_+)]^2}. \end{aligned} \quad \text{(C6)}$$

By combining all three contributions (C2), (C4), and (C6) we will get Eq. (23) in the main text. Note that discussed approximations work for $0 < h_0 < \Delta_0$.

Equation (27) can be obtained in the similar way from Eq. (25):

$$\delta\Delta(t) = \sum_p \chi_{\Delta h}(s_p) e^{s_p t} \operatorname*{Res}_{s=s_p}[\delta h(s)] + \frac{2}{\pi}\int_{\omega_-}^{\infty} \mathrm{Im}\chi_{\Delta h}(s)|_{\zeta\to+0} \mathrm{Im}[e^{i\omega t}\delta h(i\omega)]d\omega. \quad (C7)$$

The kernels $\mathcal{F}_\pm(s)$ in (26) have the same analytical properties as $\mathcal{K}_\pm(s)$ and only differ by $\mathcal{A}^2(\xi) \to \mathcal{A}(\xi)\mathcal{B}(\xi)$. The functions $\mathcal{A}$ and $\mathcal{B}$ from (B5) at the point $\xi = 0$ are

$$\mathcal{A}(0)\mathcal{B}(0) = \mathcal{A}^2(0) = \frac{(\alpha k_F)^2}{(\Delta_0 - h_0)^2}. \quad (C8)$$

Also, the analytical expressions for the kernel $\mathcal{K}_0(\omega)$ at $\omega > 0$ reads as

$$\frac{1-\mathcal{K}_0'(\omega)}{\lambda N(0)} = \begin{cases} \frac{\sqrt{4\Delta_0^2-\omega^2}}{\omega} \arctan\left(\frac{\omega}{\sqrt{4\Delta_0^2-\omega^2}}\right) & \text{for} \quad \omega < 2\Delta_0, \\ -\frac{\sqrt{\omega^2-4\Delta_0^2}}{\omega}\frac{1}{2}\ln\left(\frac{\omega-\sqrt{\omega^2-4\Delta_0^2}}{\omega+\sqrt{\omega^2-4\Delta_0^2}}\right) & \text{for} \quad \omega > 2\Delta_0, \end{cases} \quad (C9)$$

$$\frac{\mathcal{K}_0''(\omega)}{\lambda N(0)} = -\frac{\pi}{2}\frac{\sqrt{\omega^2-4\Delta_0^2}}{\omega}\Theta[\omega - 2\Delta_0]. \quad (C10)$$

Finally, the expression with the kernels $\mathcal{F}_\pm(\omega)$ from (C4) can be calculated numerically for small $\alpha k_F \ll \Delta_0$:

$$\frac{[\mathcal{F}_+'(\omega_0) - \mathcal{F}_-'(\omega_0)]}{\lambda N(0)} = h_0 \fint_0^{\omega_D} \mathcal{A}(\xi)\mathcal{B}(\xi)\frac{h_0^2 - \xi^2 - 2\Delta_0^2}{\left(\xi^2 - h_0^2\right)^2 - 4\Delta_0^2 h_0^2}d\xi. \quad (C11)$$

APPENDIX D: DERIVATION AND SOLUTION OF LZSM PROBLEM

The dynamics of two levels with avoided crossing can be simply described with the help of so-called *diabatic* basis formed by the instantaneous eigenfunction $\check{\Phi}_{kn}^0(t)$ of the time-dependent Hamiltonian (1) at $\alpha = 0$. Note here that for $\alpha = 0$ the eigenstates do not depend of $h(t)$ at all and consist only of the Bogoliubov's amplitudes u_0 and v_0 [one can use (A3) and set $\alpha = 0$ there]. The complete solution of the time-dependent Hamiltonian can be written as

$$\check{\Psi}_k(t) = \sum_n C_{kn}^d(t)\check{\Phi}_{kn}^0(t), \quad (D1)$$

where $n = \{\uparrow +, \downarrow +, \uparrow -, \downarrow -\}$. In order to avoid confusion with adiabatic basis in (28) the superscript "d" is used to denote the diabatic basis. The time-dependent coefficients obey the following equation derived from (1):

$$i\frac{\partial}{\partial t}C_m^d = \sum_n C_n^d \check{\Phi}_{km}^{0\dagger}\left[\check{\mathcal{H}}(t) - i\frac{\partial}{\partial t}\right]\check{\Phi}_{kn}^0. \quad (D2)$$

Note that here $\check{\mathcal{H}}(t)\check{\Phi}_{kn}^0 \neq E_n(t)\check{\Phi}_{kn}^0$. By keeping in mind that $\hat{\Phi}_{kn}^0(t)$ depends on time only through $\Delta(t)$, one can rewrite (D2) as follows:

$$i\frac{\partial}{\partial t}\begin{pmatrix} C_{\uparrow+}^d \\ C_{\downarrow+}^d \\ C_{\uparrow-}^d \\ C_{\downarrow-}^d \end{pmatrix} = \begin{pmatrix} E_0 - h(t) & -\frac{\xi_k}{E_0}i\alpha k e^{-i\theta_k} & i\frac{\xi_k}{2E_0^2}\frac{\partial\Delta}{\partial t} & \frac{\Delta}{E_0}i\alpha k e^{-i\theta_k} \\ \frac{\xi_k}{E_0}i\alpha k e^{i\theta_k} & E_0 + h(t) & -\frac{\Delta}{E_0}i\alpha k e^{i\theta_k} & i\frac{\xi_k}{2E_0^2}\frac{\partial\Delta}{\partial t} \\ -i\frac{\xi_k}{2E_0^2}\frac{\partial\Delta}{\partial t} & \frac{\Delta}{E_0}i\alpha k e^{-i\theta_k} & -E_0 - h(t) & \frac{\xi_k}{E_0}i\alpha k e^{-i\theta_k} \\ -\frac{\Delta}{E_0}i\alpha k e^{i\theta_k} & -i\frac{\xi_k}{2E_0^2}\frac{\partial\Delta}{\partial t} & -\frac{\xi_k}{E_0}i\alpha k e^{i\theta_k} & -E_0 + h(t) \end{pmatrix}\begin{pmatrix} C_{\uparrow+}^d \\ C_{\downarrow+}^d \\ C_{\uparrow-}^d \\ C_{\downarrow-}^d \end{pmatrix}, \quad (D3)$$

where $E_0 = \sqrt{\xi_k^2 + \Delta^2}$. One can remove the phase $\theta_k = \arg(k_x + ik_y)$ from (D3) by the unitary operator

$$\hat{U}_\theta = \begin{pmatrix} e^{i(\frac{\pi}{4}-\frac{\theta_k}{2})\hat{\sigma}_z} & 0 \\ 0 & e^{i(\frac{\pi}{4}-\frac{\theta_k}{2})\hat{\sigma}_z} \end{pmatrix}, \quad (D4)$$

so that in the new basis we have

$$i\frac{\partial}{\partial t}\begin{pmatrix} \tilde{C}_{\uparrow+}^d \\ \tilde{C}_{\downarrow+}^d \\ \tilde{C}_{\uparrow-}^d \\ \tilde{C}_{\downarrow-}^d \end{pmatrix} = \begin{pmatrix} E_0 - h(t) & -\frac{\xi}{E_0}\alpha k & i\frac{\xi}{E_0^2}\frac{\partial\Delta}{\partial t} & \frac{\Delta}{E_0}\alpha k \\ -\frac{\xi}{E_0}\alpha k & E_0 + h(t) & \frac{\Delta}{E_0}\alpha k & i\frac{\xi}{E_0^2}\frac{\partial\Delta}{\partial t} \\ -i\frac{\xi}{E_0^2}\frac{\partial\Delta}{\partial t} & \frac{\Delta}{E_0}\alpha k & -E_0 - h(t) & \frac{\xi}{E_0}\alpha k \\ \frac{\Delta}{E_0}\alpha k & -i\frac{\xi}{E_0^2}\frac{\partial\Delta}{\partial t} & \frac{\xi}{E_0}\alpha k & -E_0 + h(t) \end{pmatrix}\begin{pmatrix} \tilde{C}_{\uparrow+}^d \\ \tilde{C}_{\downarrow+}^d \\ \tilde{C}_{\uparrow-}^d \\ \tilde{C}_{\downarrow-}^d \end{pmatrix}. \quad (D5)$$

We assume that the time evolution of the gap function $\Delta(t)$ is adiabatic on the timescale of the problem (D5). Therefore, one can assume Δ to be constant during the transition with the typical time $\sim\tau_{\mathrm{LZ}}$. Since the most emphasized dynamics occurs between two crossing branches, it is convenient to consider the interaction of only the corresponding terms $C_{k\uparrow+}$ and $C_{k\downarrow-}$

(Fig. 3). Hence, one can extract an effective two-level problem for the crossing levels:

$$i\frac{\partial}{\partial t}\begin{pmatrix}\tilde{C}^d_{k\uparrow+}\\ \tilde{C}^d_{k\downarrow-}\end{pmatrix}=\begin{pmatrix}E_0-\gamma t & \frac{\Delta}{E_0}\alpha k\\ \frac{\Delta}{E_0}\alpha k & -E_0+\gamma t\end{pmatrix}\begin{pmatrix}\tilde{C}^d_{k\uparrow+}\\ \tilde{C}^d_{k\downarrow-}\end{pmatrix}. \tag{D6}$$

This system can be viewed as the LZSM problem, which allows an exact solution [36]. However, as discussed in Sec. IV B, one can neglect the transient dynamics of the $C_k(t)$ coefficients in the gap equation (3) and use the transition matrix approach instead. Thus, we need to obtain the relation between the long-time asymptotes of the functions $\tilde{C}^d_{k\uparrow\downarrow+}(t)$ before (t_0-) and after (t_0+) transition at the point $t_0(\xi_k)=\sqrt{\xi_k^2+\Delta^2}/\gamma$. Here we use short notations $(t_0\mp)\approx t_0\mp\tau_{\rm LZ}/2$. The asymptotic solution of the problem (D6) is well known [36] and reads as

$$\begin{pmatrix}\tilde{C}^d_{k\uparrow+}(t_0+)\\ \tilde{C}^d_{k\downarrow-}(t_0+)\end{pmatrix}=\begin{pmatrix}\sqrt{p_k} & -\mathrm{sgn}(\alpha)\sqrt{1-p_k}e^{i\chi_k}\\ \mathrm{sgn}(\alpha)\sqrt{1-p_k}e^{-i\chi_k} & \sqrt{p_k}\end{pmatrix}\begin{pmatrix}\tilde{C}^d_{k\uparrow+}(t_0-)\\ \tilde{C}^d_{k\downarrow-}(t_0-)\end{pmatrix}, \tag{D7}$$

where the coefficient

$$p_k=\exp\left[-\delta_{\rm LZ}\frac{\Delta^2}{\xi_k^2+\Delta^2}\right]$$

with $\delta_{\rm LZ}=\pi\alpha^2k^2/\gamma\approx\pi\alpha^2k_F^2/\gamma$ defines the probability of tunneling. Here $\chi_k=\pi/4+\arg\Gamma(1+i\ln p_k/2\pi)-\ln p_k[\ln(-\ln p_k/2\pi)-1]/2\pi$ is the Stokes phase with the gamma function Γ.

For small energies $\xi_k\lesssim\Delta$ two different tunneling regimes are possible:

$$\text{(weak)}\quad \gamma\gtrsim\alpha^2k_F^2\to\delta_{\rm LZ}\approx 0\to p_k\approx 1,$$
$$\text{(strong)}\quad \gamma\ll\alpha^2k_F^2\to\delta_{\rm LZ}\gg 1\to p_k\approx 0.$$

When $\xi_k\gg\Delta$, tunneling is suppressed ($p_k\to 1$) as the quasiparticle spectrum resembles that of a normal metal with no splitting between crossing spectral branches.

The typical transient time $\tau_{\rm LZ}$ for the LZSM tunneling can be estimated as follows [36]:

$$\tau_{\rm LZ}\sim\sqrt{\frac{\hbar}{\gamma}}\max\left\{1,\frac{\alpha k_F}{\sqrt{2\gamma}}\frac{\Delta}{\sqrt{\xi_k^2+\Delta^2}}\right\}.$$

If the intersection of the branches of the QP spectrum occurs at some ξ_k, then it is possible to determine the interval $\Delta\xi_k$ in which all QP states experience transient dynamics. The size of $\Delta\xi_k$ depends on transient time, however, it can be shown that the upper limit for this interval is $\Delta\xi_k\sim\alpha k_F\ll\Delta$. The smallness of $\Delta\xi_k$ and the fact that the gap function $\Delta(t)$ is determined by all QP states in $(-\omega_D,\omega_D)$ confirm the validity of the approximations made in Sec. IV B.

Combining all the results we write the asymptotic transition matrix $\hat{S}^d_{\rm LZ}$ in diabatic basis as

$$\begin{pmatrix}C^d_{k\uparrow+}(t_0+)\\ C^d_{k\downarrow+}(t_0+)\\ C^d_{k\uparrow-}(t_0+)\\ C^d_{k\downarrow-}(t_0+)\end{pmatrix}=\begin{pmatrix}\sqrt{p_k} & 0 & 0 & \sqrt{1-p_k}e^{i\chi_k-i\theta_k-i\frac{\pi}{2}\mathrm{sgn}(\alpha)}\\ 0 & 1 & 0 & 0\\ 0 & 0 & 1 & 0\\ -\sqrt{1-p_k}e^{-i\chi_k+i\theta_k+i\frac{\pi}{2}\mathrm{sgn}(\alpha)} & 0 & 0 & \sqrt{p_k}\end{pmatrix}\begin{pmatrix}C^d_{k\uparrow+}(t_0-)\\ C^d_{k\downarrow+}(t_0-)\\ C^d_{k\uparrow-}(t_0-)\\ C^d_{k\downarrow-}(t_0-)\end{pmatrix}. \tag{D8}$$

The LZSM transition matrix in the adiabatic basis (28) has the form $\hat{S}_{\rm LZ}=\hat{R}^{-1}(t_0+)\hat{S}^d_{\rm LZ}\hat{R}(t_0-)$, where we use the relationship between the two bases (D1) and (28) written in general form as a time-dependent matrix $\hat{R}(t)$. Using the perturbation theory with respect to the small parameter $\alpha k_F/\Delta$ and considering points $t_0\pm$ far from the nonadiabatic region, one can show that the matrix $\hat{R}(t_0\pm)$ can be approximated with an identity matrix. The corrections proportional to $\alpha k_F/\Delta$ in all elements of the matrix $\hat{R}(t_0\pm)$ as well as $\hat{S}_{\rm LZ}$ can be neglected since in all equations of Sec. IV we consider the minimum possible order of the perturbation theory with respect to the parameter $\alpha k_F/\Delta$. With these approximations the matrices $\hat{S}_{\rm LZ}$ and $\hat{S}^d_{\rm LZ}$ actually coincide and the LZSM transition matrix in the adiabatic basis can be taken taken from (D8). Thus, we get Eq. (32).

APPENDIX E: CALCULATION OF SPIN-SPLIT DOS

The DOS for one spin projection can be written as follows:

$$N_\uparrow(E,t)\approx\sum_k\sum_{n=\uparrow+,\uparrow-}|u_0|^2\delta(E-E_{kn})+|v_0|^2\delta(E+E_{kn}). \tag{E1}$$

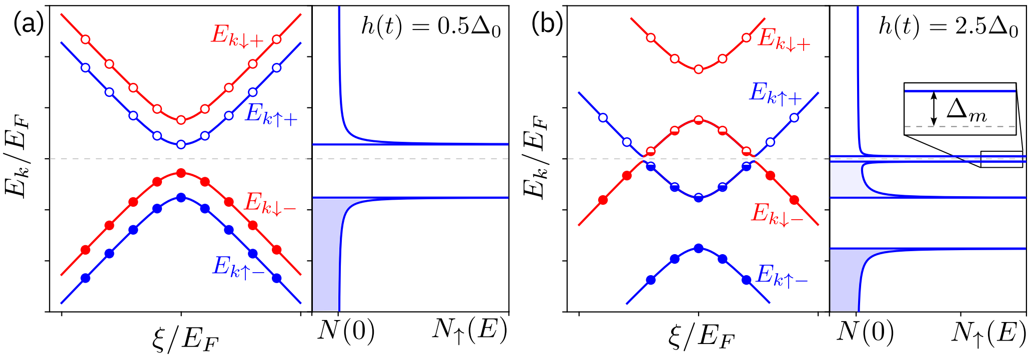

FIG. 6. Spectrum (4) and density of states (E2)–(E4) for the QPs with ↑ spin for two different values of $h(t)$. The value Δ_m represents a minigap. Colored areas in DOS indicate the filling of the states in the corresponding energy intervals according to Eq. (45). The parameters are $\Delta_0/E_F = 0.01$, $\alpha/E_F = 0.0025$.

Here we use static QP amplitudes u_0 and v_0 to distinguish the particle and hole contributions and $E_{k\uparrow\pm}$ are defined in Eq. (4). Note that the function $N_\uparrow(E,t)$ depends on time only through the Zeeman field $h(t)$. The straightforward calculations for $h(t) < \Delta_0$ yield

$$\frac{N_\uparrow(E,t)}{N(0)} \approx \frac{|E|}{\xi_0}\left|1 - \mathrm{sgn}(E)\frac{\alpha^2k_F^2 + h^2(t)}{\sqrt{\xi_0^2\alpha^2k_F^2 + h^2(t)\left(\xi_0^2 + \Delta_h^2\right)}}\right|^{-1}, \tag{E2}$$

where

$$\xi_0(E,t) \approx \sqrt{E^2 + h^2(t) - \Delta_h^2 + \alpha^2k_F^2 + \mathrm{sgn}(E)2\sqrt{E^2\left(h^2(t) + \alpha^2k_F^2\right) - \Delta_h^2\alpha^2k_F^2}} \tag{E3}$$

and we have assumed $\alpha k \approx \alpha k_F$ due to the vicinity to the Fermi energy. The time-dependent gap function $\Delta_h[h(t)]$ is defined in (38). Two standard coherence peaks at the energies $E = -\sqrt{(\Delta_h + h(t))^2 + \alpha^2k_F^2}$ and $E = \sqrt{(\Delta_h - h(t))^2 + \alpha^2k_F^2}$ appear [Fig. 6(a)].

For the case of large Zeeman fields $h(t) > \Delta_0$ one obtains

$$\frac{N_\uparrow(E,t)}{N(0)} \approx \begin{cases} \frac{|E|}{\xi_0}\left|1 - \mathrm{sgn}(E)\frac{\alpha^2k_F^2+h^2(t)}{\sqrt{\xi_1^2\alpha^2k_F^2+h^2(t)(\xi_1^2+\Delta_h^2)}}\right|^{-1}, & E > \Delta_m \quad \text{and} \quad E < -\sqrt{(\Delta_h + h(t))^2 + \alpha^2k_F^2}, \\ \frac{|E|}{\xi_0}\left|1 - \frac{\alpha^2k_F^2+h^2(t)}{\sqrt{\xi_2^2\alpha^2k_F^2+h^2(t)(\xi_2^2+\Delta_h^2)}}\right|^{-1}, & -\sqrt{(\Delta_h - h(t))^2 + \alpha^2k_F^2} < E < -\Delta_m, \end{cases} \tag{E4}$$

where

$$\Delta_m \approx \frac{\Delta_h\alpha k_F}{\sqrt{h^2(t) + \alpha^2k_F^2}}.$$

The splitting of the energy spectrum in the vicinity of $E = 0$ leads to the appearance of the two additional coherence peaks and corresponding minigap at the energies $E = \pm\Delta_m$, which are shown in Fig. 6(b).

[1] D. Langenberg, A. Larkin, and A. Larkin, *Nonequilibrium Superconductivity*, Modern problems in condensed matter sciences (North-Holland, Amsterdam, 1986).

[2] N. Kopnin, *Theory of Nonequilibrium Superconductivity*, International Series of Monographs on Physics (Clarendon, Oxford, 2001).

[3] A. F. Volkov and S. M. Kogan, Collisionless relaxation of the energy gap in superconductors, Sov. J. Exper. Theor. Phys. **38**, 1018 (1974).

[4] I. O. Kulik, O. Entin-Wohlman, and R. Orbach, Pair susceptibility and mode propagation in superconductors: A microscopic approach, J. Low Temp. Phys. **43**, 591 (1981).

[5] P. W. Higgs, Broken Symmetries and the Masses of Gauge Bosons, Phys. Rev. Lett. **13**, 508 (1964).

[6] D. Pekker and C. Varma, Amplitude/Higgs modes in condensed matter physics, Annu. Rev. Condens. Matter Phys. **6**, 269 (2015).

[7] A. Moor, A. F. Volkov, and K. B. Efetov, Amplitude Higgs Mode and Admittance in Superconductors with a Moving Condensate, Phys. Rev. Lett. **118**, 047001 (2017).

[8] S. Nakamura, Y. Iida, Y. Murotani, R. Matsunaga, H. Terai, and R. Shimano, Infrared Activation of the Higgs Mode by Supercurrent Injection in Superconducting NbN, Phys. Rev. Lett. **122**, 257001 (2019).

[9] M. Bellitti, C. R. Laumann, and B. Z. Spivak, Incoherent excitation of coherent Higgs oscillations in superconductors, Phys. Rev. B **105**, 104513 (2022).

[10] T. Papenkort, V. M. Axt, and T. Kuhn, Coherent dynamics and pump-probe spectra of BCS superconductors, Phys. Rev. B **76**, 224522 (2007).

[11] R. Matsunaga, N. Tsuji, H. Fujita, A. Sugioka, K. Makise, Y. Uzawa, H. Terai, Z. Wang, H. Aoki, and R. Shimano, Light-induced collective pseudospin precession resonating with Higgs mode in a superconductor, Science **345**, 1145 (2014).

[12] R. Matsunaga, Y. I. Hamada, K. Makise, Y. Uzawa, H. Terai, Z. Wang, and R. Shimano, Higgs Amplitude Mode in the BCS Superconductors $Nb_{1-x}Ti_xN$ Induced by Terahertz Pulse Excitation, Phys. Rev. Lett. **111**, 057002 (2013).

[13] A. F. Kemper, M. A. Sentef, B. Moritz, J. K. Freericks, and T. P. Devereaux, Direct observation of Higgs mode oscillations in the pump-probe photoemission spectra of electron-phonon mediated superconductors, Phys. Rev. B **92**, 224517 (2015).

[14] R. Shimano and N. Tsuji, Higgs mode in superconductors, Annu. Rev. Condens. Matter Phys. **11**, 103 (2020).

[15] A. I. Buzdin, Proximity effects in superconductor-ferromagnet heterostructures, Rev. Mod. Phys. **77**, 935 (2005).

[16] M. Eschrig, Spin-polarized supercurrents for spintronics: a review of current progress, Rep. Prog. Phys. **78**, 104501 (2015).

[17] T. T. Heikkilä, M. Silaev, P. Virtanen, and F. S. Bergeret, Thermal, electric and spin transport in superconductor/ferromagnetic-insulator structures, Prog. Surf. Sci. **94**, 100540 (2019).

[18] M. Houzet, Ferromagnetic Josephson Junction with Precessing Magnetization, Phys. Rev. Lett. **101**, 057009 (2008).

[19] S. E. Barnes, M. Aprili, I. Petković, and S. Maekawa, Ferromagnetic resonance with a magnetic josephson junction, Supercond. Sci. Technol. **24**, 024020 (2011).

[20] I. Petković, M. Aprili, S. E. Barnes, F. Beuneu, and S. Maekawa, Direct dynamical coupling of spin modes and singlet josephson supercurrent in ferromagnetic Josephson junctions, Phys. Rev. B **80**, 220502(R) (2009).

[21] S. Takahashi, S. Hikino, M. Mori, J. Martinek, and S. Maekawa, Supercurrent Pumping in Josephson Junctions with a Half-Metallic Ferromagnet, Phys. Rev. Lett. **99**, 057003 (2007).

[22] L.-L. Li, Y.-L. Zhao, X.-X. Zhang, and Y. Sun, Possible evidence for spin-transfer torque induced by spin-triplet supercurrents*, Chin. Phys. Lett. **35**, 077401 (2018).

[23] I. A. Golovchanskiy, N. N. Abramov, O. V. Emelyanova, I. V. Shchetinin, V. V. Ryazanov, A. A. Golubov, and V. S. Stolyarov, Magnetization Dynamics in Proximity-Coupled Superconductor-Ferromagnet-Superconductor Multilayers. II. Thickness Dependence of the Superconducting Torque, Phys. Rev. Appl. **19**, 034025 (2023).

[24] M. Silaev, Anderson-Higgs Mass of Magnons in Superconductor-Ferromagnet-Superconductor Systems, Phys. Rev. Appl. **18**, L061004 (2022).

[25] V. L. Vadimov, I. M. Khaymovich, and A. S. Mel'nikov, Higgs modes in proximized superconducting systems, Phys. Rev. B **100**, 104515 (2019).

[26] G. Tang, W. Belzig, U. Zülicke, and C. Bruder, Signatures of the Higgs mode in transport through a normal-metal–superconductor junction, Phys. Rev. Res. **2**, 022068(R) (2020).

[27] S. V. Mironov and A. I. Buzdin, Collective magnetic and plasma excitations in josephson ψ junctions, Phys. Rev. B **104**, 134502 (2021).

[28] Y. Lu, S. Ilić, R. Ojajärvi, T. T. Heikkilä, and F. S. Bergeret, Reducing the frequency of the Higgs mode in a helical superconductor coupled to an LC-circuit, arXiv:2212.11615.

[29] M. A. Silaev, R. Ojajärvi, and T. T. Heikkilä, Spin and charge currents driven by the Higgs mode in high-field superconductors, Phys. Rev. Res. **2**, 033416 (2020).

[30] Y. Lu, R. Ojajärvi, P. Virtanen, M. A. Silaev, and T. T. Heikkilä, Coupling the Higgs mode and ferromagnetic resonance in spin-split superconductors with Rashba spin-orbit coupling, Phys. Rev. B **106**, 024514 (2022).

[31] G. Sarma, On the influence of a uniform exchange field acting on the spins of the conduction electrons in a superconductor, J. Phys. Chem. Solids **24**, 1029 (1963).

[32] A. Abrikosov, *Fundamentals of the Theory of Metals* (Dover, New York, 2017).

[33] S. Tewari, T. D. Stanescu, J. D. Sau, and S. D. Sarma, Topologically non-trivial superconductivity in spin–orbit-coupled systems: bulk phases and quantum phase transitions, New J. Phys. **13**, 065004 (2011).

[34] J. Ketterson, J. Ketterson, S. Song, and K. B, *Superconductivity* (Cambridge University Press, Cambridge, 1999).

[35] P. Z. Genwang Fan and Xiao-Long Chen, Probing two Higgs oscillations in a one-dimensional fermi superfluid with raman-type spin-orbit coupling, Front. Phys. **17**, 52502 (2022).

[36] O. V. Ivakhnenko, S. N. Shevchenko, and F. Nori, Nonadiabatic Landau-Zener-Stückelberg-Majorana transitions, dynamics, and interference, Phys. Rep. **995**, 1 (2023).

[37] A. Behrle, T. Harrison, J. Kombe, K. Gao, M. Link, J.-S. Bernier, C. Kollath, and M. Köhl, Higgs mode in a strongly interacting fermionic superfluid, Nat. Phys. **14**, 781 (2018).

[38] P. Wang, W. Yi, and G. Xianlong, Topological phase transition in the quench dynamics of a one-dimensional fermi gas with spin-orbit coupling, New J. Phys. **17**, 013029 (2015).

[39] Y. Dong, L. Dong, M. Gong, and H. Pu, Dynamical phases in quenched spin–orbit-coupled degenerate Fermi gas, Nat. Commun. **6**, 6103 (2015).

[40] K. V. Samokhin, Goldstone modes in Larkin-Ovchinnikov-Fulde-Ferrell superconductors, Phys. Rev. B **81**, 224507 (2010).

[41] Z. Huang, C. S. Ting, J.-X. Zhu, and S.-Z. Lin, Gapless Higgs mode in the Fulde-Ferrell-Larkin-Ovchinnikov state of a superconductor, Phys. Rev. B **105**, 014502 (2022).

[42] L. P. Gor'kov and E. I. Rashba, Superconducting 2D System with Lifted Spin Degeneracy: Mixed Singlet-Triplet State, Phys. Rev. Lett. **87**, 037004 (2001).

[43] Note that here we focus on the problem with a single pairing channel. The collective modes in systems with several pairing channels may be of interest in the context of theoretical and experimental studies of multicomponent superconductors and superfluids. In particular, in a helium system the breaking of complex symmetry (including gauge transformation as well as spin and orbital rotations) by the matrix order parameter leads to the appearance of multiple Higgs modes [52,53].

[44] P. A. Frigeri, D. F. Agterberg, and M. Sigrist, Spin susceptibility in superconductors without inversion symmetry, New J. Phys. **6**, 115 (2004).

[45] D. B. Szombati, S. Nadj-Perge, D. Car, S. R. Plissard, E. P. A. M. Bakkers, and L. P. Kouwenhoven, Josephson

ϕ-junction in nanowire quantum dots, Nat. Phys. **12**, 568 (2016).

[46] A. Kirilyuk, A. V. Kimel, and T. Rasing, Ultrafast optical manipulation of magnetic order, Rev. Mod. Phys. **82**, 2731 (2010).

[47] A. Kirilyuk, A. V. Kimel, and T. Rasing, Laser-induced magnetization dynamics and reversal in ferrimagnetic alloys, Rep. Prog. Phys. **76**, 026501 (2013).

[48] A. El-Ghazaly, J. Gorchon, R. B. Wilson, A. Pattabi, and J. Bokor, Progress towards ultrafast spintronics applications, J. Magn. Magn. Mater. **502**, 166478 (2020).

[49] E. Gershenzon, M. Gershenzon, G. Gol'tsman, A. Lyul'kin, A. Semenov, and A. Sergeev, Electron-phonon interaction in ultrathin Nb films, Sov. Phys.–JETP **70**, 505 (1990).

[50] A. Kardakova, M. Finkel, D. Morozov, V. Kovalyuk, P. An, C. Dunscombe, M. Tarkhov, P. Mauskopf, T. M. Klapwijk, and G. Goltsman, The electron-phonon relaxation time in thin superconducting titanium nitride films, Appl. Phys. Lett. **103**, 252602 (2013).

[51] S. Tsuchiya, D. Yamamoto, R. Yoshii, and M. Nitta, Hidden charge-conjugation, parity, and time-reversal symmetries and massive Goldstone (Higgs) modes in superconductors, Phys. Rev. B **98**, 094503 (2018).

[52] G. Volovik and M. Zubkov, Higgs bosons in particle physics and in condensed matter, J. Low Temp. Phys. **175**, 486 (2014).

[53] V. Zavjalov, S. Autti, V. Eltsov, P. Heikkinen, and G. Volovik, Light higgs channel of the resonant decay of magnon condensate in superfluid ^{3}He-B, Nat. Commun. **7**, 10294 (2016).